NASA/CR—2004-212718

Advanced Subsonic Technology (AST) 22-Inch Low Noise Research Fan Rig Preliminary Design of ADP-Type Fan 3

David A. Topol, Clint L. Ingram, and Michael J. Larkin
United Technologies Corporation, Pratt & Whitney, East Hartford, Connecticut

Charles H. Roche and Robert D. Thulin
FTS, Inc., East Hartford, Connecticut

February 2004

The NASA STI Program Office . . . in Profile

Since its founding, NASA has been dedicated to the advancement of aeronautics and space science. The NASA Scientific and Technical Information (STI) Program Office plays a key part in helping NASA maintain this important role.

The NASA STI Program Office is operated by Langley Research Center, the Lead Center for NASA's scientific and technical information. The NASA STI Program Office provides access to the NASA STI Database, the largest collection of aeronautical and space science STI in the world. The Program Office is also NASA's institutional mechanism for disseminating the results of its research and development activities. These results are published by NASA in the NASA STI Report Series, which includes the following report types:

- TECHNICAL PUBLICATION. Reports of completed research or a major significant phase of research that present the results of NASA programs and include extensive data or theoretical analysis. Includes compilations of significant scientific and technical data and information deemed to be of continuing reference value. NASA's counterpart of peer-reviewed formal professional papers but has less stringent limitations on manuscript length and extent of graphic presentations.

- TECHNICAL MEMORANDUM. Scientific and technical findings that are preliminary or of specialized interest, e.g., quick release reports, working papers, and bibliographies that contain minimal annotation. Does not contain extensive analysis.

- CONTRACTOR REPORT. Scientific and technical findings by NASA-sponsored contractors and grantees.

- CONFERENCE PUBLICATION. Collected papers from scientific and technical conferences, symposia, seminars, or other meetings sponsored or cosponsored by NASA.

- SPECIAL PUBLICATION. Scientific, technical, or historical information from NASA programs, projects, and missions, often concerned with subjects having substantial public interest.

- TECHNICAL TRANSLATION. English-language translations of foreign scientific and technical material pertinent to NASA's mission.

Specialized services that complement the STI Program Office's diverse offerings include creating custom thesauri, building customized databases, organizing and publishing research results . . . even providing videos.

For more information about the NASA STI Program Office, see the following:

- Access the NASA STI Program Home Page at ***http://www.sti.nasa.gov***

- E-mail your question via the Internet to help@sti.nasa.gov

- Fax your question to the NASA Access Help Desk at 301–621–0134

- Telephone the NASA Access Help Desk at 301–621–0390

- Write to:
  NASA Access Help Desk
  NASA Center for AeroSpace Information
  7121 Standard Drive
  Hanover, MD 21076

NASA/CR—2004-212718

Advanced Subsonic Technology (AST) 22-Inch Low Noise Research Fan Rig Preliminary Design of ADP-Type Fan 3

David A. Topol, Clint L. Ingram, and Michael J. Larkin
United Technologies Corporation, Pratt & Whitney, East Hartford, Connecticut

Charles H. Roche and Robert D. Thulin
FTS, Inc., East Hartford, Connecticut

Prepared under Contract NAS3–27727

National Aeronautics and
Space Administration

Glenn Research Center

February 2004

Acknowledgments

Acknowledgements are given to the following persons for their contributions to this task:

NASA Glenn Research Center

Project Manager	Dennis Huff
Task Manager	Robert J. Jeracki
Data Analysis	Christopher J. Miller

Pratt & Whitney, East Hartford, CT

CFD Validation	Clint L. Ingram
Acoustics	David A. Topol
Fan Aerodynamics	Robert Neubert
Rig Airflow Analysis	Mike J. Larkin
Task Management	Walt Brockett

Belcan (Contractor to P&W)

FEGV Aerodynamics	William Crabtree, Len Noryk

FTS, East Hartford, CT (Contractor to P&W)

Structural Analysis	Charles H. Roche
Report Preparation	Robert D. Thulin

Available from

NASA Center for Aerospace Information
7121 Standard Drive
Hanover, MD 21076

National Technical Information Service
5285 Port Royal Road
Springfield, VA 22100

Available electronically at http://gltrs.grc.nasa.gov

FOREWORD

This report presents the results of work completed on the preliminary design of Fan 3 as part of NASA's 22-in. Fan Low Noise Research project. Fan 3 was intended to build on the experience gained from Fans 1 and 2 by demonstrating noise reduction technology that surpasses 1992 levels by 6 dB.

The work was performed within the auspices of NASA's Advanced Subsonic Technology (AST) program, and under Contract NAS3-27727 – *Critical Propulsion and Noise Reduction Technologies for Future Commercial Subsonic Engines*; *Task 14.1: 22-in. Rig Program.*

ABSTRACT

This NASA AST task was authorized to design and build the third fan (Fan 3) in a series of 22-in. diameter tip fan rigs for NASA testing at GRC. Fan 1 and Fan 2 were two low tip speed fans designed and tested as part of the NASA Large Engine Technology (LET) program under Contract NAS3-26618. This advanced high-bypass ratio (BPR) rig (Fan 3) was intended to build on the experience gained from Fan 1 and Fan 2 and demonstrate noise reduction technology that surpassed 1992 levels by 6 dB.

Fan 1 and Fan 2 both featured variable pitch advanced ducted propulsor (ADP) rotors designed for tip speeds of 840 and 756 ft/sec, respectively. The testing showed that Fan 2, although expected to be 2 dB quieter than Fan 1, was found to be 1.7, 1.4 and -0.1 dB noisier for sideline, cutback, and approach, respectively.

Work on this task was conducted in the areas of computational fluid dynamics (CFD) code validation: acoustic prediction and validation; rotor parametric studies and fan exit guide vane (FEGV) studies, up to the time when a NASA decision was made to cancel the design; fabrication; and testing phases of the work. The decision was based on financial concerns and the realization that similar information would be obtained from another 22-in. rig program. The scope of the program changed accordingly to concentrate on two subtasks:

1. Rig data analysis and CFD code validation
2. Fan and FEGV optimization studies.

The results of the CFD code validation work showed that this tool predicts three-dimensional (3-D) flowfield features well from approximately the blade trailing edge to a chord downstream. The CFD tool loses accuracy as the distance from the trailing edge increases beyond a blade chord.

The comparisons of noise predictions to rig test data showed that both the tone noise tool (TFaNS) and the broadband noise tool (BFaNS) demonstrated reasonable agreement with the data to the degree that these tools can be used reliably for design work.

Fan 1 and Fan 2 test data was analyzed for noise differences since the expected 2 dB noise reduction for Fan 2 was not realized. The scaling rules used for this prediction were:

- The standard 50 log (tip speed) scaling factor for the reduced tip speed of Fan 2, which indicated a reduction of 2.5 dB
- The empirical 7 log (vane number) scaling factor from Boeing rig testing for broadband noise, which predicted a 0.4 dB increase.

The result was a net 2 dB broadband noise reduction. When using the BFaNS to evaluate Fan 2 the results confirm a noise increase on the order of 2 dB. These results show that the scaling rules initially used do not apply to the different aerodynamic loading of these two fans.

The section on rig airflow and inlet separation analysis describes the method used to determine total fan airflow and shows the good agreement of predicted boundary layer profiles to measured profiles. The results of the inlet flow separation studies show separation angles of attack ranging from 29.5 degrees to 27 degrees for the range of airflows tested.

The results of the rotor parametric studies were significant in leading to the decision not to pursue a new rotor design for Fan 3. Noise predictions for a 750 ft/sec Fan 3 rotor showed little reduction compared to Fan 2, resulting in recommendations to concentrate efforts on FEGV stator designs. The ensuing parametric study on FEGV designs showed the potential for 8 to 10 EPNdB noise reduction relative to the baseline, with the configuration featuring 22 bowed vanes with 30 degrees of sweep demonstrating the greatest potential.

A preliminary rig nacelle structural analysis was performed on the 22-vane configuration, bowed with 30 degrees of sweep, relative to the 52-vane configuration of Fan 1. The results showed the 22-vane configuration to be significantly stiffer than the original in the torsional and axial directions and only slightly stiffer in the transverse direction. Stress results were not determined due to cancellation of this part of the program.

CONTENTS

FIGURES

TABLES

ACRONYMS

Numerics

1-D	One Dimensional
2-D	Two Dimensional
3-D	Three Dimensional

A

ADP	Advanced Ducted Propulsor
APP	Approach
AST	Advanced Subsonic Technology
At	Inlet Throat Area

B

BFaNS	Broadband Noise Tool
BPF	Blade Passing Frequency
BPR	Bypass Ratio

C

C/B	Cutback
CFD	Computational Fluid Dynamics

E

EPNL	Effective Perceived Noise Level

F

FEGV	Fan Exit Guide Vane

G

GRC	Glenn Research Center

I

ID	Inner Diameter

L

LDV	Laser Doppler Velocimetry
LET	Large Engine Technology

O

OD	Outer Diameter

P

P&W	Pratt & Whitney

S

S/L	Sideline

T

TFaNS	Tone Noise Tool
TOGW	Takeoff Gross Weight
TDC	Top Dead Center

U

UTRC	United Technologies Research Center

1. INTRODUCTION

Major airports in the nation's air transportation system face a serious problem in providing greater capacity to meet the ever increasing demands of air travel. This problem could be relieved if airports are allowed to increase their operating time, now restricted by curfews, and by relaxing present limits on takeoffs and landings. A key operational issue and feature in the argument against the extension of the present curfews is noise.

In response to increasingly restrictive noise regulations, NASA is conducting a noise reduction project as part of the AST program. The goal of the project is to reduce the noise level of aircraft by a cumulative 30 dB, relative to 1992 technology, by the end of the decade. This implies noise reduction of 10 dB in each of three aircraft flight phases where aircraft noise is measured: takeoff, sideline, and approach.

As part of noise reduction efforts in the fan section of aircraft engines, NASA has conducted rig testing on a 22-in. fan/nacelle model. Two low tip speed fans with 22-in. diameter tip were designed and tested as part of this program. Reference 17 describes the design of a low noise fan stage (Fan 1) and Reference 11 describes the design of an advanced low noise fan stage (Fan 2). Both fans were variable pitch ADP rotors designed for tip speeds of 840 and 756 ft/sec respectively. The testing, which was performed at NASA GRC, included acoustic, aerodynamic, and structural tests. Fan 2, although expected to be 2 dB quieter than Fan 1, was found to be nosier by 1.7, 1.4, and -0.1 dB for sideline, cutback, and approach, respectively.

The purpose of this report is to document the work completed for Fan 3. The initial purpose of this task was to demonstrate further noise reductions than those demonstrated in Fan 1 and Fan 2, to achieve a noise objective of 6 dB less than 1992 levels. After program initiation, work in the areas of CFD code validation, acoustic prediction and validation, rotor parametric studies, and FEGV studies were conducted up to the time when a NASA decision was made to cancel the design, fabrication, and testing phases of this task. The decision was based on financial concerns and the realization that similar information would be obtained from another 22-in. rig program. After the cancellation, the purpose of this task became one of validating CFD codes for fan aerodynamics and developing fan acoustic prediction tools.

In view of the above cancellation decision, the following work was completed:

- Data analysis and code validation
  - — CFD code validation involving comparisons of predicted-to-measured aerodynamic parameters for P&W's large scale (5 ft) research rig, the NASA/Allison 22-in. rig, and Fan 1.
  - — Acoustic predictions of Fan 1 noise using aerodynamic test data.
  - — Acoustic predictions of Fan 1 noise using predicted aerodynamic data.
  - — Analysis of noise differences between Fan 1 and Fan 2 data.
  - — 22-in. rig nacelle aerodynamic analysis involving CFD predicted boundary layer analysis compared to measured test data, and an analysis of inlet distortion data to determine separation angle of attack.
- Fan Design Optimization Studies
  - — Parametric design study of basic aerodynamic drivers of noise for selected rotor configurations.
  - — FEGV parametric study to determine the drivers of noise for five stator vane configurations.
  - — Structural analysis of the most promising FEGV configuration from the parametric study.

The results of the work done in this task are significant for advancing the development of fan noise prediction tools. The predictions made for Fan 3, using the results from Fan 1 and Fan 2, were influential in focusing efforts on the FEGV, rather than on rotor characteristics.

2. DATA ANALYSIS AND CODE VALIDATION

2.1 COMPARISONS OF CFD PREDICTIONS TO RIG TEST DATA

P&W's 3-D CFD capability has been applied to three related fan configurations to understand the physics of how the aerodynamic flowfield causes noise. The CFD code has been assessed by comparing mean wake profiles and turbulence predictions with available measured wake profiles and turbulence properties from United Technologies Research Center's (UTRC's) 5-ft rig, Allison Engine Company's (Allisons's) 22-in. fan,[1] and the P&W/NASA 22-in. Fan 1. P&W's CFD code is a cell centered pressure-based Navier-Stokes implicit flow solver with a k-$\in$ turbulence model (Reference 1 and 2). These three fan designs were chosen to aid in determining what factors are involved in accurately predicting wakes. It is believed that the three fan designs represent an adequate cross section of data, speeds, and geometry.

CFD predictions were performed on UTRC's large scale 5 ft research rig to provide low tip speed fan data for the evaluation of code accuracy. The UTRC rig was chosen because the measurement probe rotates with the rotor. This assisted in determining the contribution of unsteady flow behavior by comparing CFD (relative frame) to phase locked laser doppler velocimetry (LDV) measured wakes.

The Allison test data from the 22-in. fan was used to provide an initial assessment of P&W's ability to predict rotor wakes. NASA provided rotor and endwall geometry, inlet total pressure, total temperature, and gas angles as a function of radius to be used as CFD boundary conditions. NASA provided the reported pressure ratio and efficiency, as well as exit profiles, of pressure ratio, temperature ratio, and efficiency for near stall, a single point on the fan map. P&W provided the predicted rotor exit wakes information prior to seeing the Allison test data and NASA made the comparisons to data in order to provide an objective assessment of P&W's predictive capability. The Allison 22-in. fan was ideal, since noise and wake data at three different stations was available.

CFD predictions were performed on the P&W/NASA 22-in. Fan 1 to provide a broader base of relevant low tip speed fan data for evaluation of code accuracy. The profiles, wakes, and turbulence of the ADP Fan 1 rotor were predicted and compared to test results. This 22-in. fan was ideal, since noise and wake data at two stations were available, with the second located over two chords downstream of the fan trailing edge.

2.1.1 CFD Motivation and Background

CFD accuracy requirements for a noise prediction system are higher than for an aerodynamic design system. In the past, the fan designers were mostly interested in accurately predicting one-dimensional (1-D) and two-dimensional (2-D) fan performance, such as pressure ratio and efficiency. Today, as noise moves up near the top of priorities in fan design, accurate predictions of wake shapes, turbulence mixing, and other 3-D flow details become a priority. The goal of this task is two-fold: to assess and improve the prediction capability of such flow features and to gain understanding of fan noise sources like wakes and turbulence so that low noise fans can be designed.

[1] Allison is a Rolls-Royce company.

2.1.2 UTRC 5-ft Rig

Three flows were modeled (65, 85, and 95 percent axial velocity over the average of leading and trailing edge rotational velocities, or *Cx/Um*), and wake profile comparisons were completed at a 50 percent span. ***Figure 2-1*** illustrates the CFD model of the rig and shows wake profile comparison locations (labeled *Station 1*). Comparisons at 50 percent span and 10 percent chord downstream of the trailing edge are shown in ***Figure 2-2***. The comparisons show the CFD model to accurately predict the wake shape (deficit and width). Unfortunately, data at other locations has been lost and comparisons cannot be made. It is not known how well the model compares near the inner diameter (ID) and outer diameter (OD) of the flowpath and a chord or two downstream. The wake comparisons in ***Figure 2-2*** would indicate, however, that the blade losses are accurately predicted. While data was acquired from 10 to 110 percent chord aft of the rotor at various incidences, the data is not accessible. Therefore, it is not possible to determine if the difference between predicted wakes and data is primarily due to phase-locking errors in the measurements.

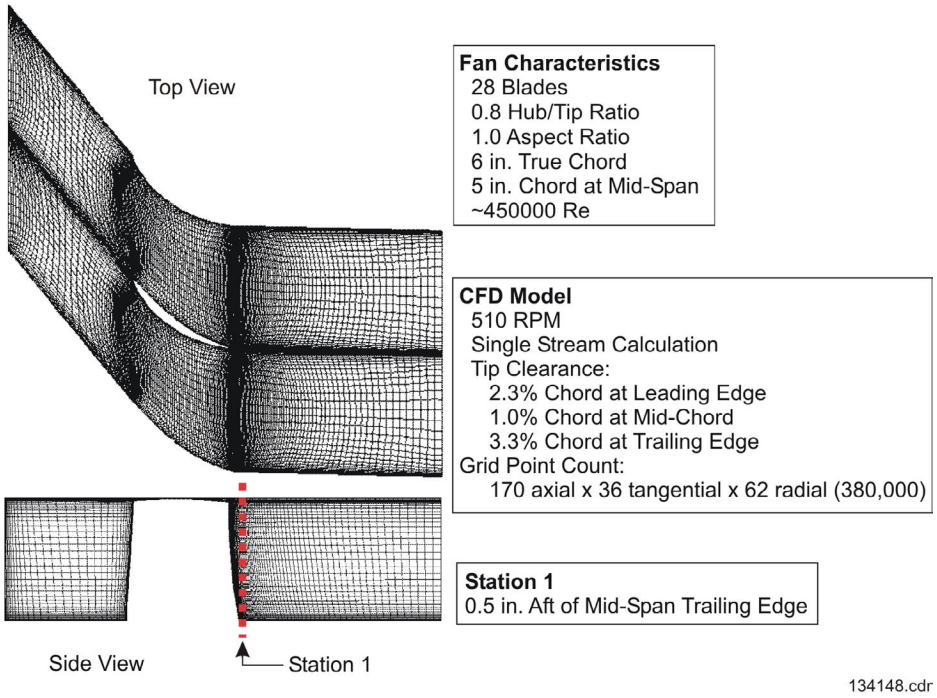

Figure 2-1. *The CFD Model of the UTRC 5-ft Rig*

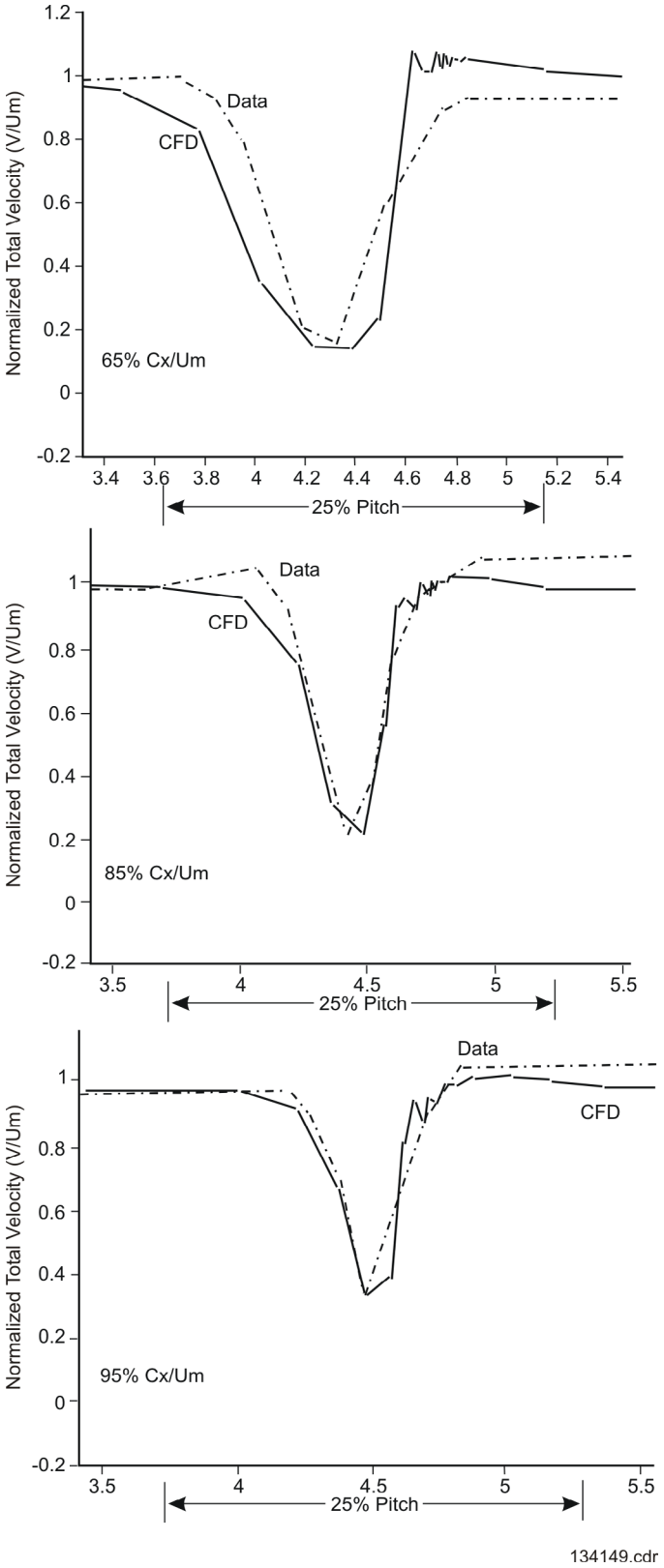

Figure 2-2. *Wake Comparisons (50 Percent Span) at Station 1 of UTRC 5-ft Rig*

2.1.3 Allison 22-in. Fan

This Allison 22-in. fan is an ideal fan for study, since noise and wake data at three different stations is available. NASA provided all the necessary input for creating the CFD model (geometry, boundary conditions, and data) and P&W supplied CFD results to NASA for data comparison. ***Figure 2-3*** illustrates the details of the CFD model and shows the locations of the LDV data stations, with the furthest from the fan trailing edge located about a chord away.

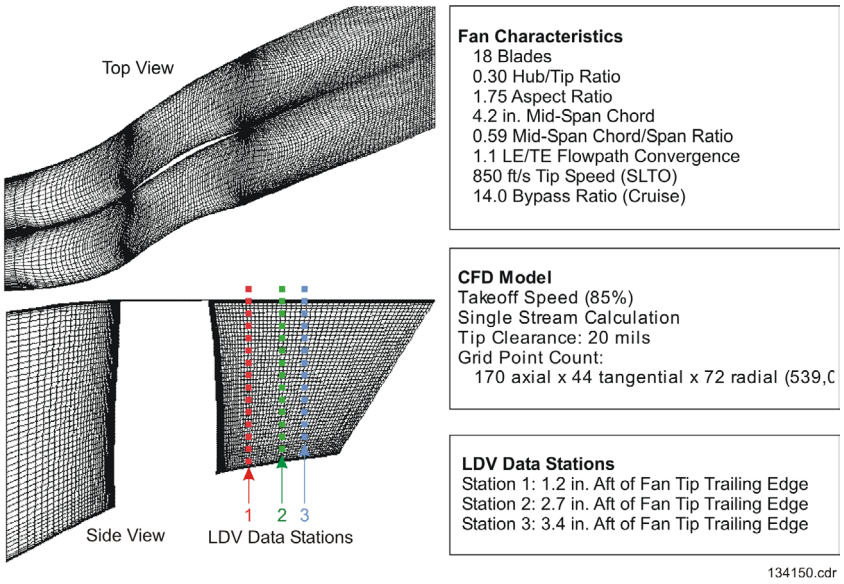

Figure 2-3. *The CFD Model of the Allison 22-in. Fan*

NASA delivered the geometry, boundary conditions, and radial distributions of pressure ratio, temperature ratio, and efficiency at near stall, a single point on the map. ***Figure 2-4*** shows where the comparison of the CFD model to data is performed on the map characteristic.

Figure 2-5 shows the comparison of the CFD model to radial distributions of pressure ratio, temperature ratio, and efficiency at a data point. The CFD model compared very well to data at Station 2, matching both the level and shape of the profiles. Even the level of overshoot in the temperature ratio near the OD was predicted well. ***Figure 2-6*** shows the wakes at the three stations through two parameters: the axial component of the velocity and the turbulent kinetic energy. Comparisons of CFD model wakes to data wakes were performed and show excellent agreement out to Station 3 (about one chord downstream of the rotor trailing edge). The results, shown in ***Figure 2-7*****,** show good agreement of wake deficit and width, from 14 to 79 percent span.

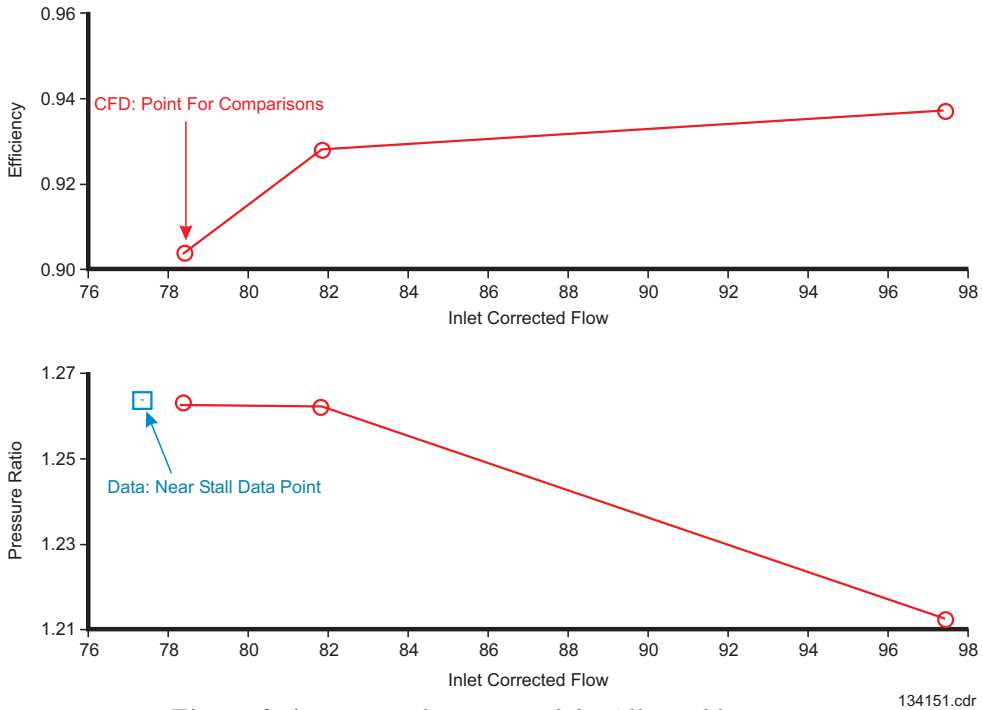

Figure 2-4. *Fan Performance of the Allison 22-in. Fan*

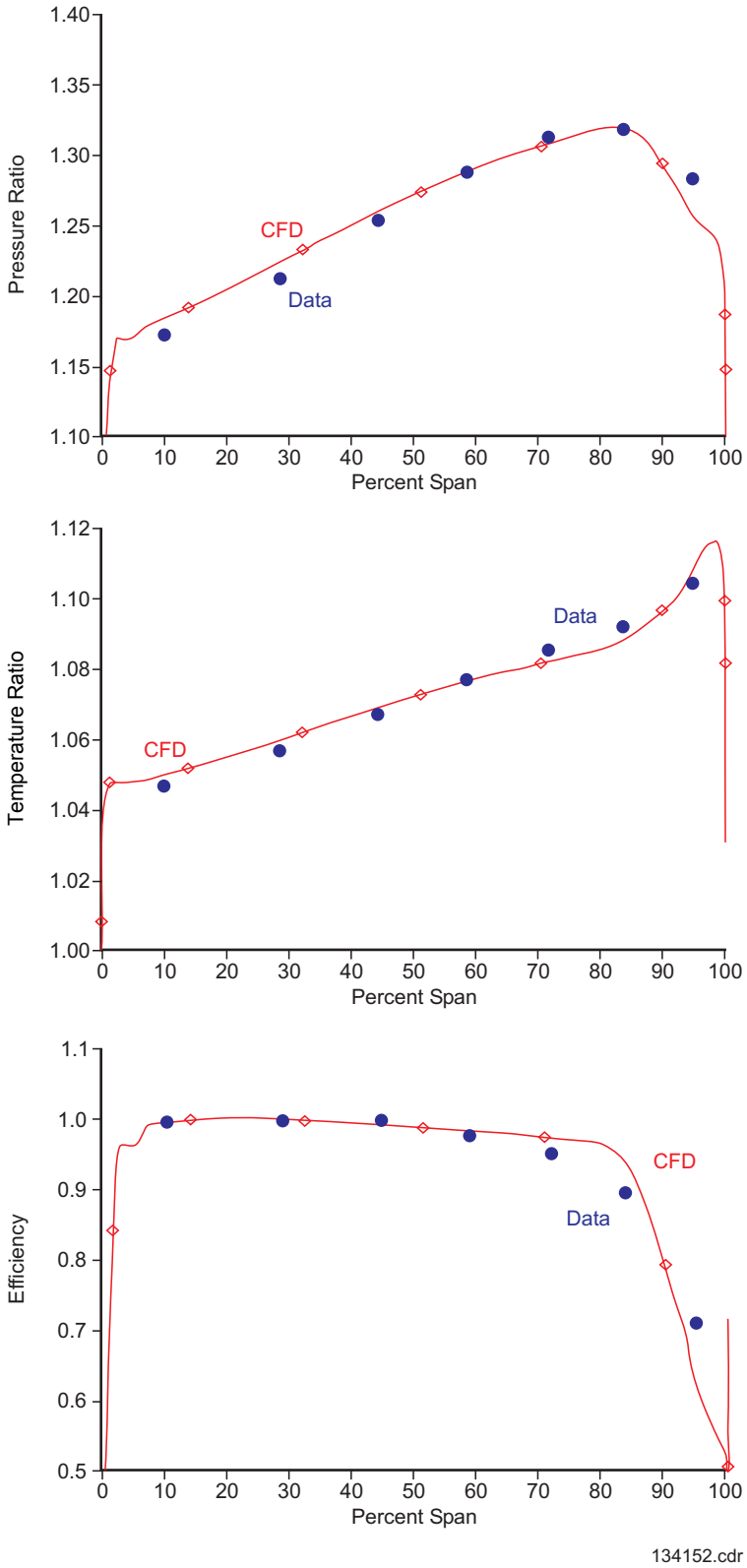

Figure 2-5. *Radial Profile Comparisons at Station 2 of the Allison 22-in. Fan*

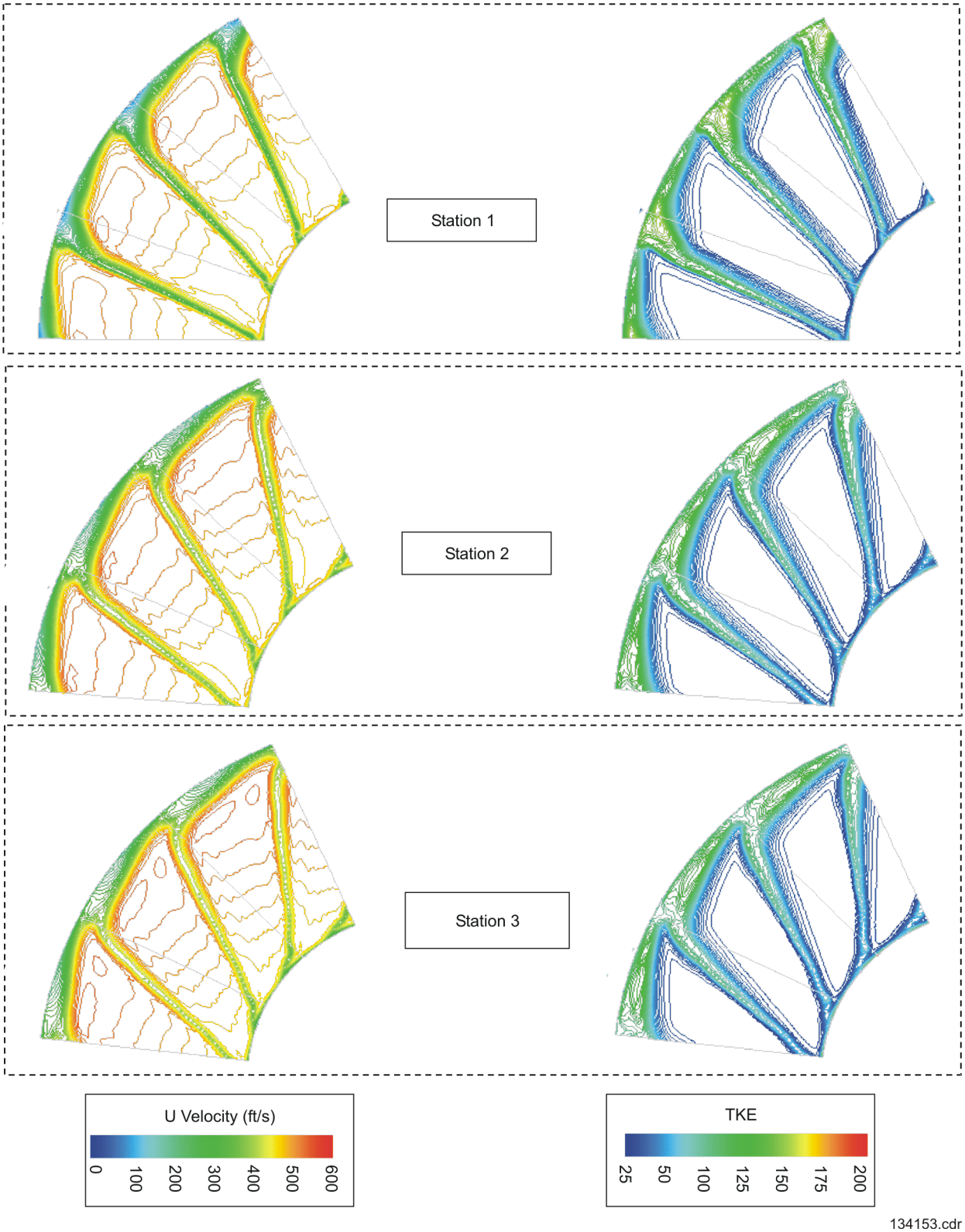

Figure 2-6. *CFD Prediction for the Allison 22-in. Fan*

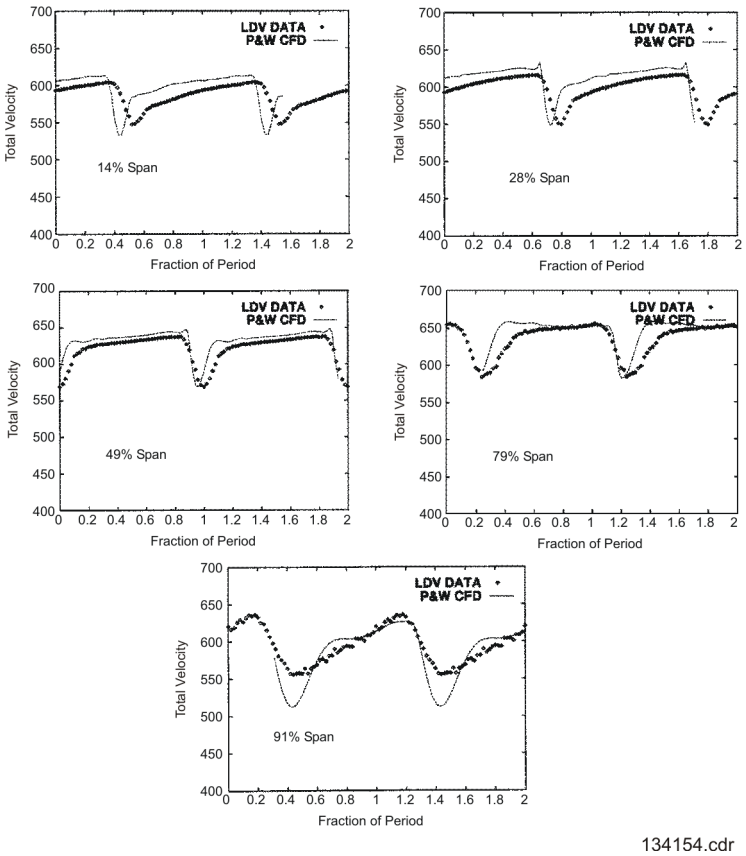

Figure 2-7. *Wake Comparisons at Station 3 of the Allison 22-in. Fan (As Reported By NASA)*

2.1.4 ADP 22-in. Fan 1

The 22-in. Fan 1 is an ideal case to study, because both noise and wake data at two stations downstream of the rotor are taken. ***Figure 2-8*** shows the data stations and all the relevant information describing the CFD model, as well as the fan characteristics. Since these predictions are input to the fan noise prediction models, accuracy of the full 3-D nature of the flowfield, such as fan wake size and shape and turbulence, are extremely important. In order to obtain the best match to data, several modeling issues became extremely important. The 3-D wake shapes were dependent on bypass ratio, modeling of the fan hub gap, correct tip clearance, grid wake resolution, and turbulence transition modeling. All these parameters were specified to produce the best CFD/data match.

Figure 2-9 shows where the CFD model to data comparison is performed on the map characteristic. The point of comparison is near the operating line and close to the point at which data was obtained. The comparison of the CFD model to data for radial distributions of pressure ratio, temperature ratio, and efficiency are shown in ***Figures 2-10*** and ***2-11. Figure 2-10*** shows the comparisons in the core; ***Figure 2-11*** shows the comparisons in the duct. There is a small miss in the CFD model prediction in the core. ***Figure 2-11*** also shows errors in the data as well; it is impossible to have efficiencies greater than 1.0, as the figure suggests.

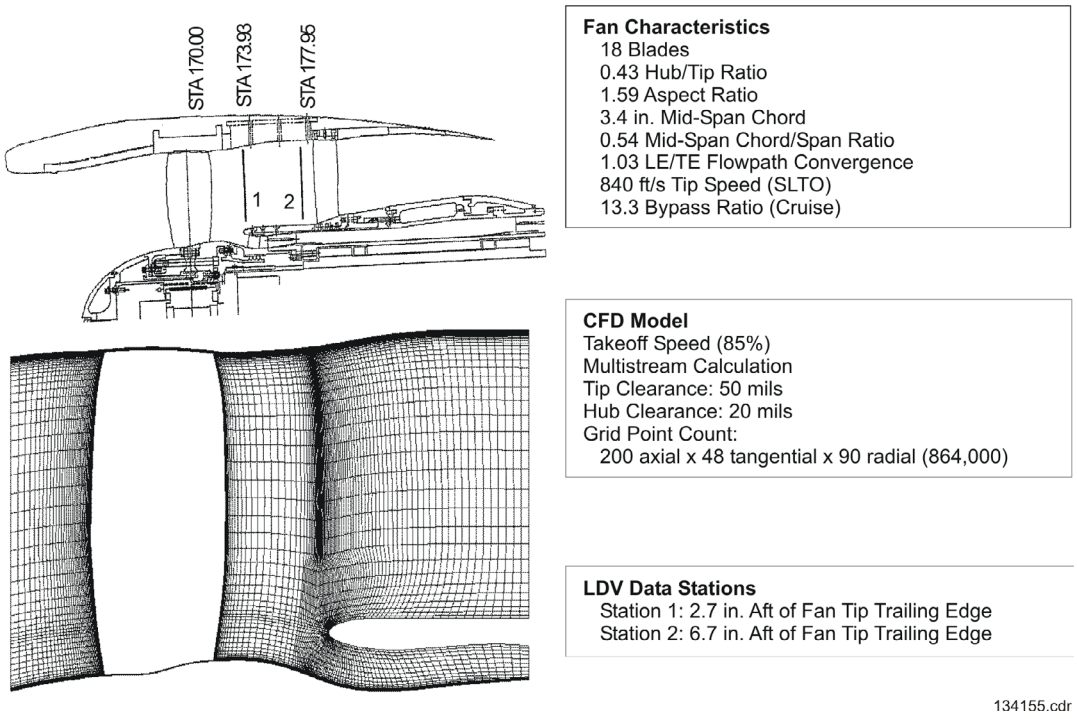

Figure 2-8. *The CFD Model of the ADP 22-in. Fan 1*

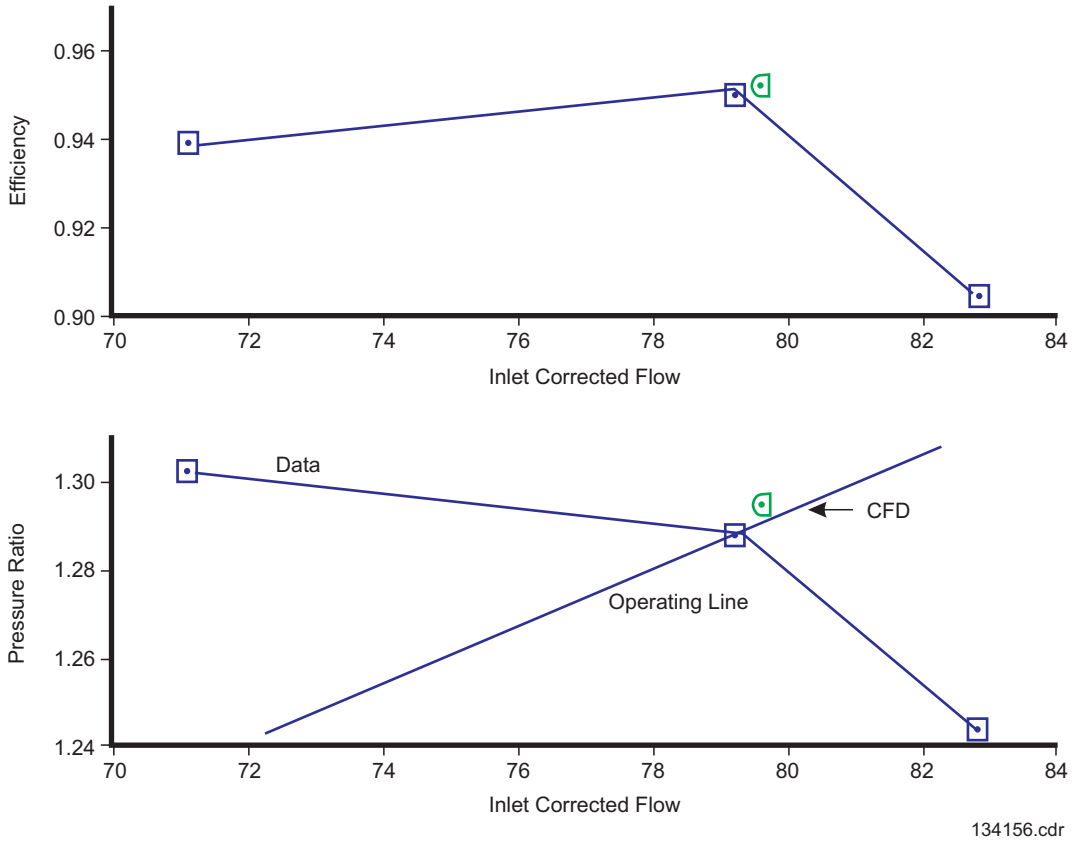

Figure 2-9. *Fan Performance of the ADP 22-in. Fan 1*

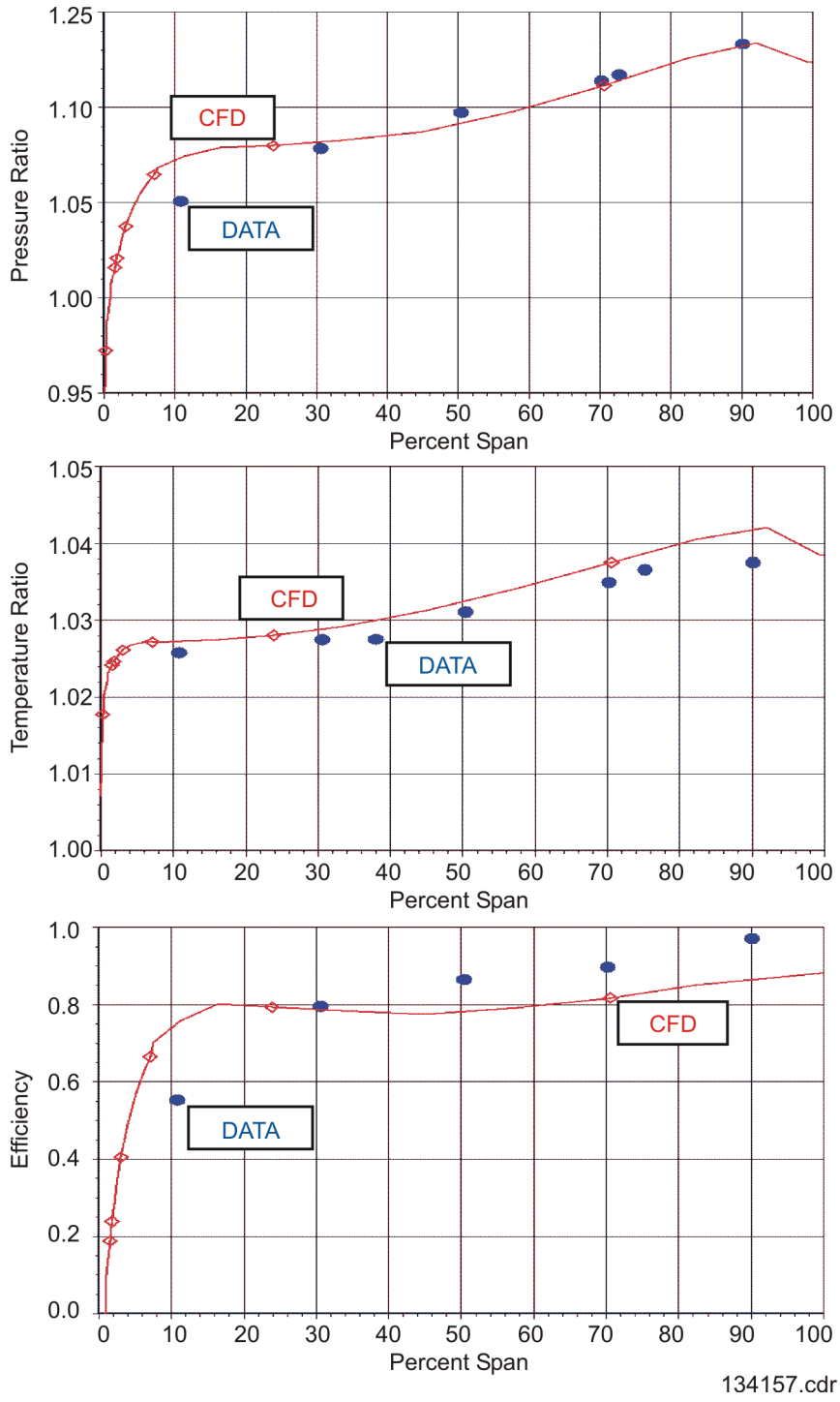

Figure 2-10. *Radial Profile Comparisons at Stator Leading Edge of the ADP 22-in. Fan 1 Core*

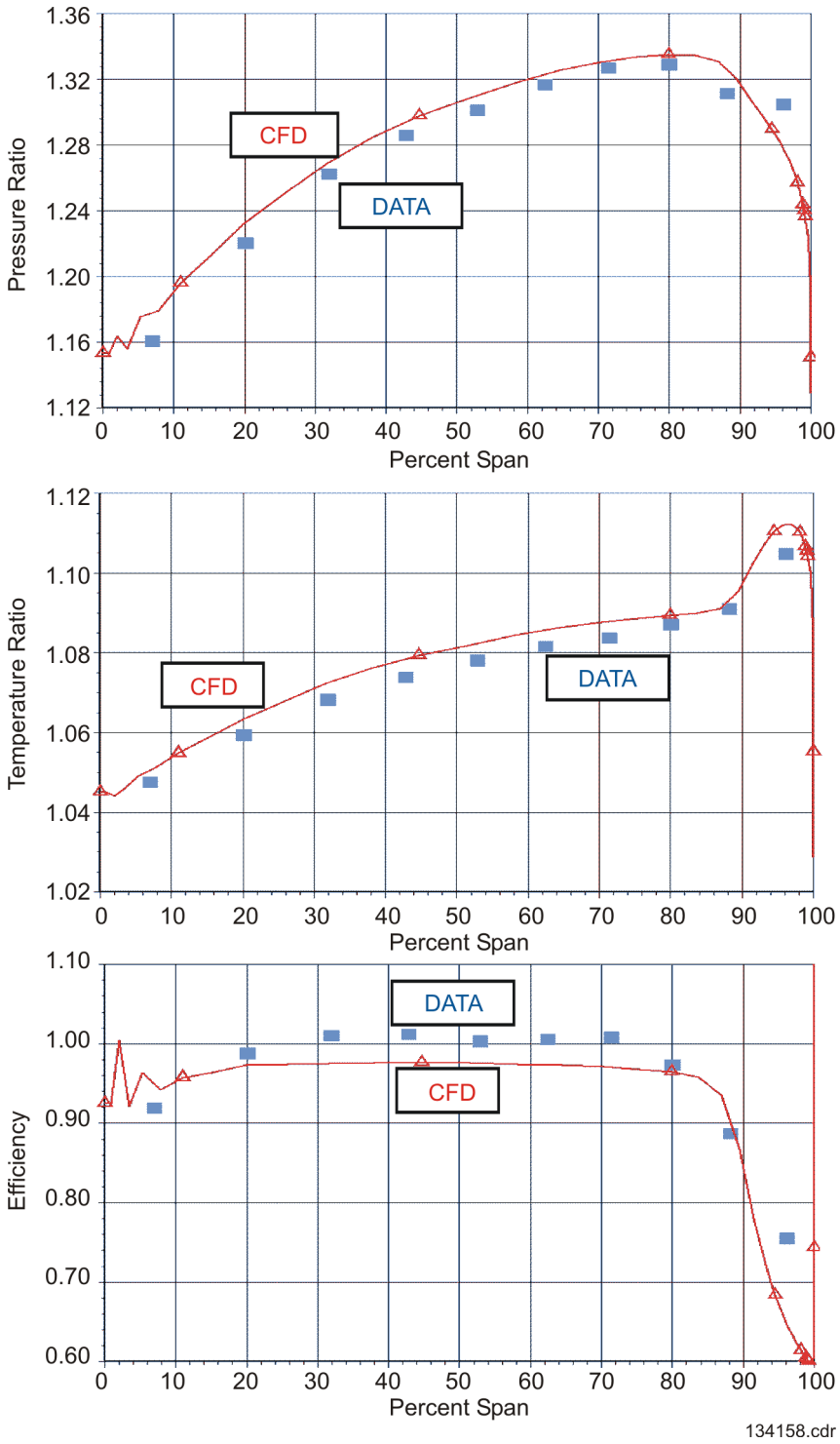

Figure 2-11. *Radial Profile Comparisons at Station 12.5 of the ADP 22-in. Fan 1*

The comparisons of 1-D and 2-D CFD models to data of overall properties indicate the CFD model is adequate for fan performance predictions. However, for noise prediction, further comparisons must be performed to provide insight into the 3-D predictive capability for wakes and turbulence. ***Figures 2-12*** and ***2-13*** show the wakes at Stations 1 and 2 through five parameters: the absolute, relative, and upwash velocity (perpendicular velocity to the mean) and the absolute and relative air angles. These parameters are essential for accurate prediction of tone noise and were compared qualitatively to determine wake phasing and shape. The CFD model obtains a reasonable prediction of these properties, as evidenced by the accurate prediction of the radially-curved shape of the wakes at both stations. However, ***Figure 2-13*** (illustrating the flow through the duct) shows a mismatch between CFD model and data near the splitter (ID of the duct) and the OD of the duct.

Figures 2-14 and ***2-15*** show comparisons of the CFD model to data of the wake deficit and width at Stations 1 and 2 and various span locations. The comparison at Station 1 (about one chord downstream of the rotor trailing edge) shows generally good agreement. The CFD model is in excellent agreement with data for the width of the wake in the midspan region, but the depth of the wake is overpredicted. In the hub region, the wake width is considerably underpredicted. These results are similar to the results obtained by Chima (Reference 3). The comparison at Station 2 (about two chords downstream of the rotor trailing edge) shows worse agreement. The comparison in ***Figure 2-15*** shows ID and OD discrepancies and misses in wake depth at midspan.

Further investigation showed the CFD models to more closely match data when a separation forms over the splitter leading edge. This information was obtained by modeling half of the experimentally measured core flow. While this flow change is physically unlikely, it is useful to investigate these results. ***Figures 2-16*** and ***2-17*** show comparisons of the CFD models to data of the wake deficit and width at Stations 1 and 2 for half of the core flow. These figures illustrate better agreement with data near the splitter at Station 2. The midspan to OD wake shapes were not affected. ***Figure 2-18*** illustrates how halving the core flow incurs a separation over the splitter leading edge. Once the separation forms, the profiles in the core and the duct compared better between CFD model and data.

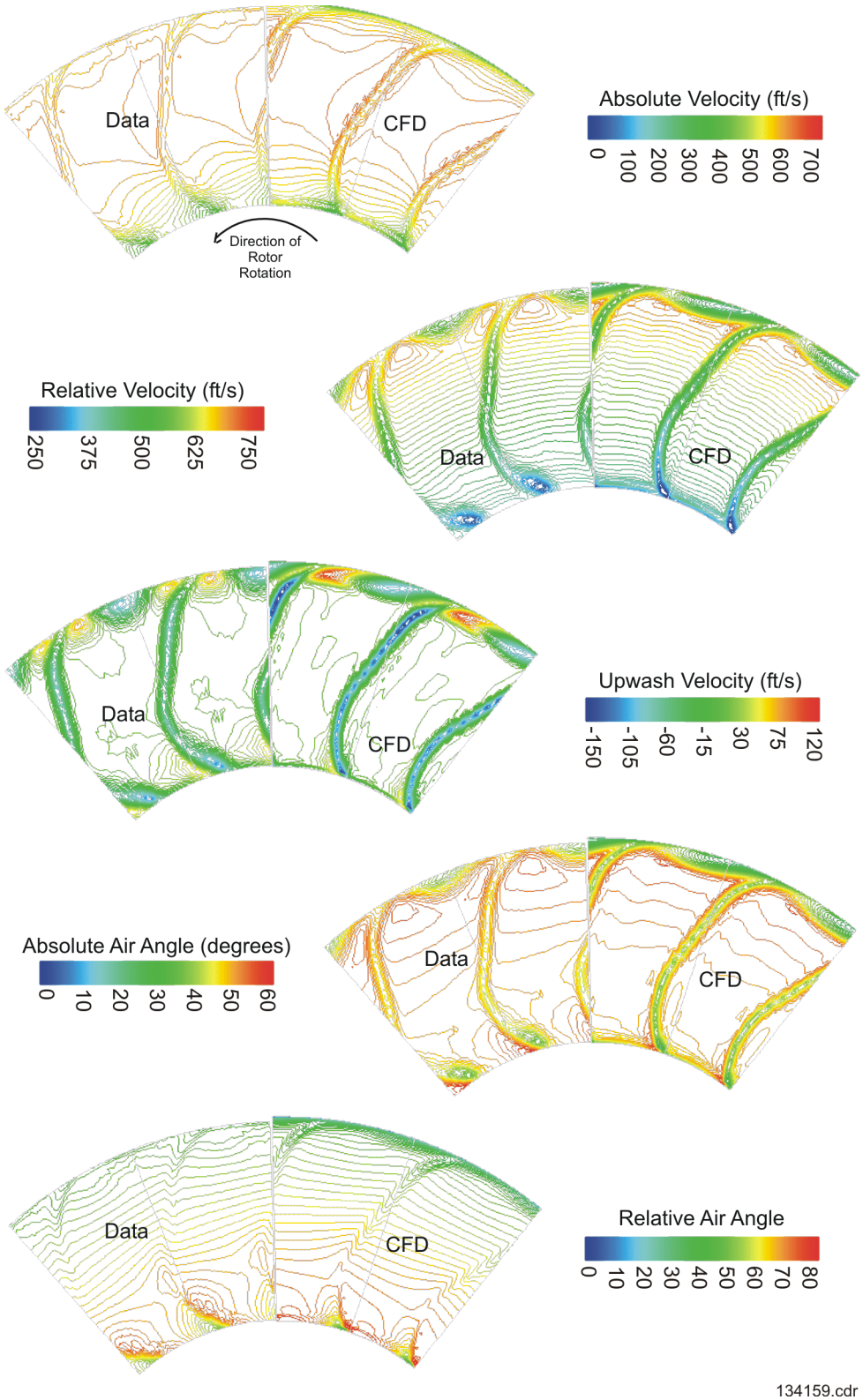

Figure 2-12. *Comparison of CFD Prediction to Data at Station 1 of ADP 22-in. Fan 1*

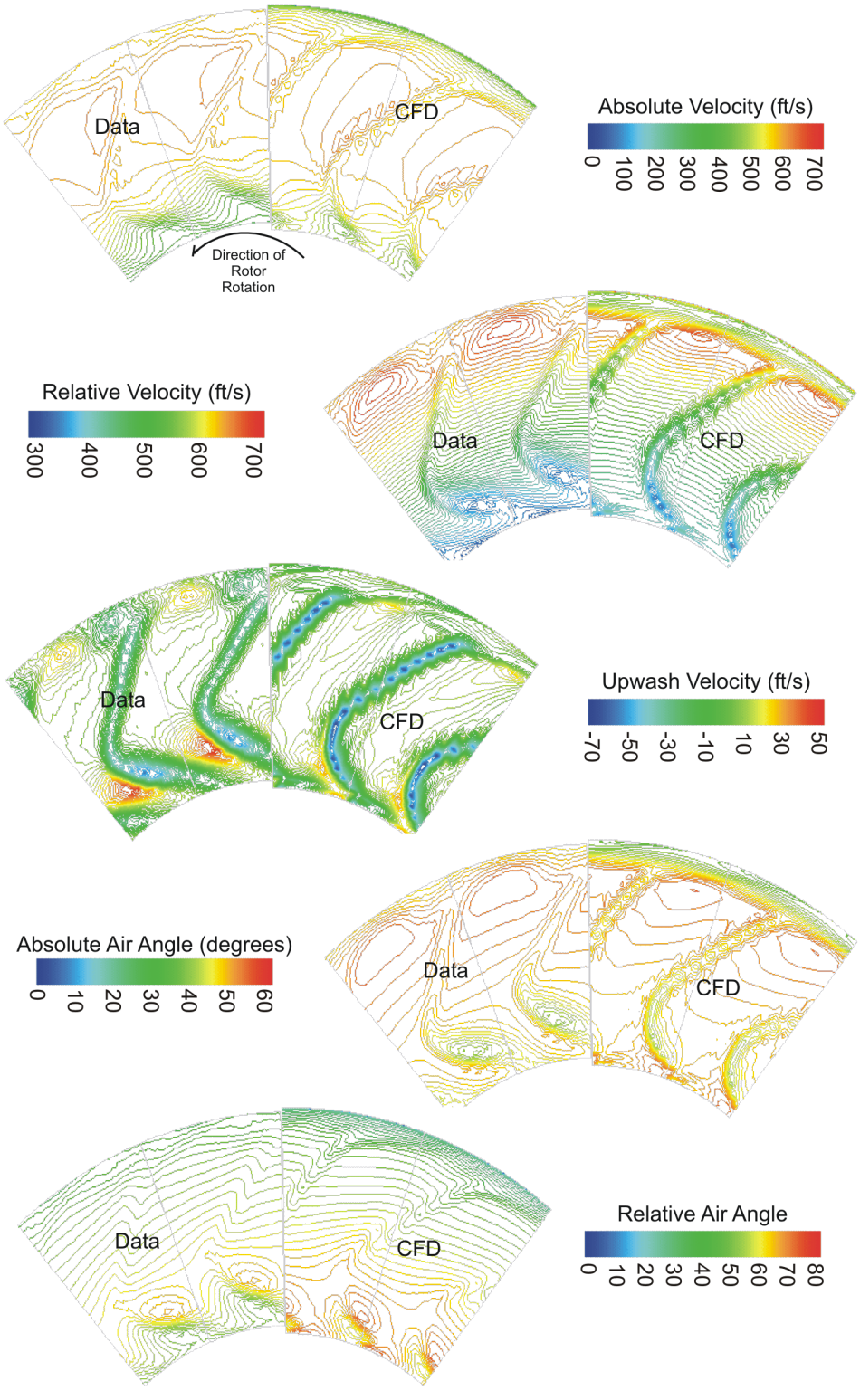

Figure 2-13. *Comparison of CFD Prediction to Data at Station 2 of ADP 22-in. Fan 1*

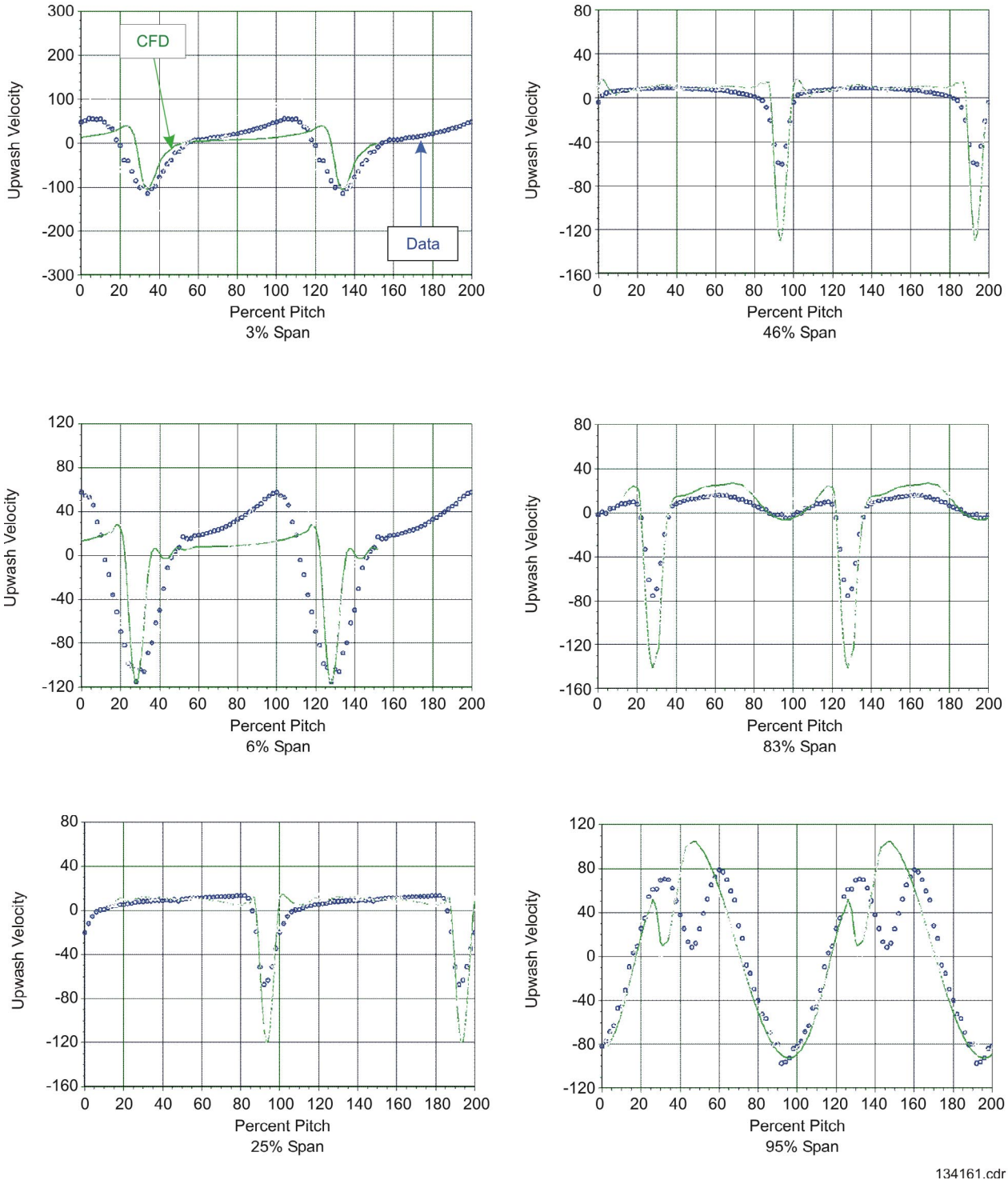

Figure 2-14. *Wake Comparisons at Station 1 of the ADP 22-in. Fan*

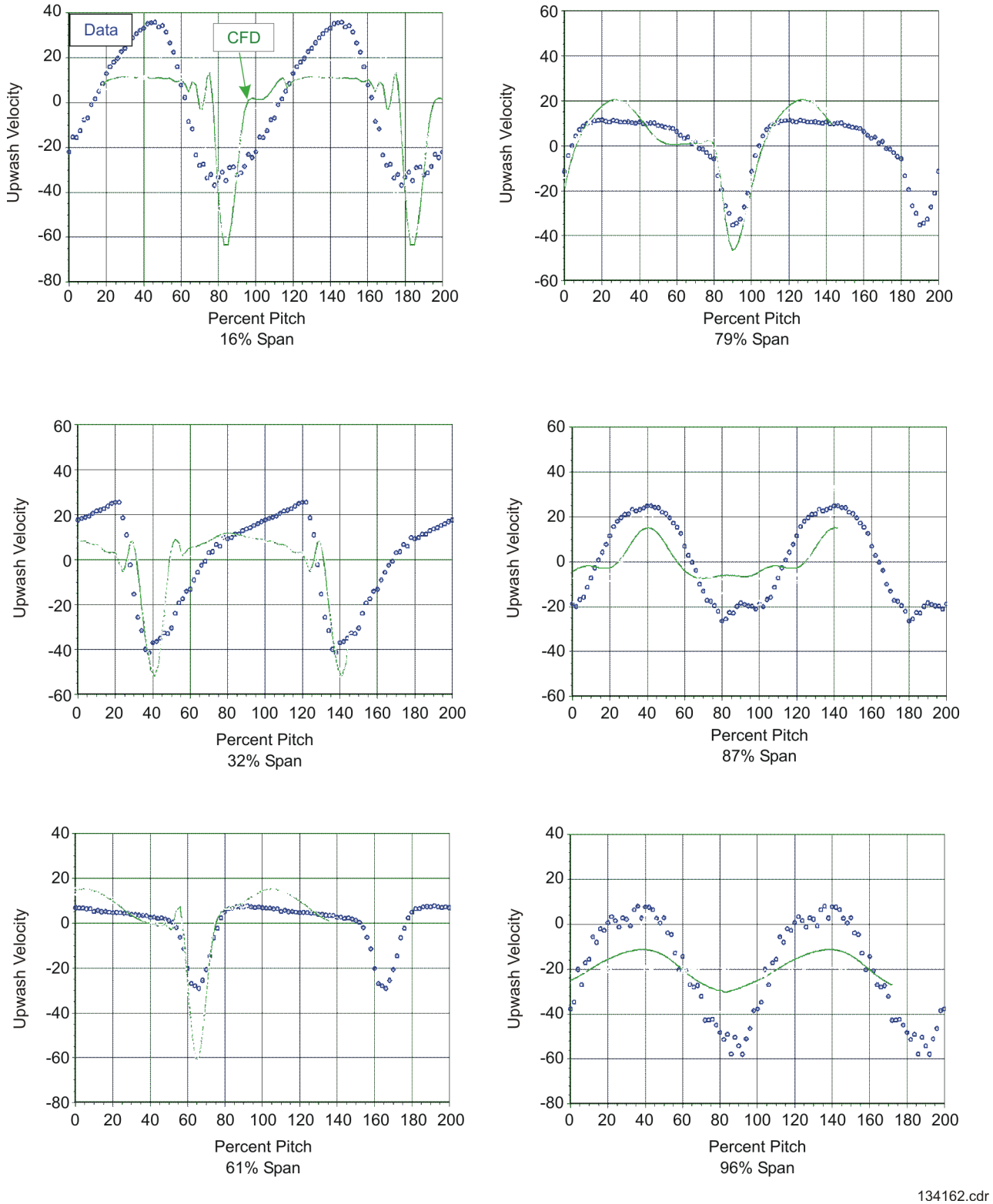

Figure 2-15. *Wake Comparison at Station 2 of the ADP 22-in. Fan 1*

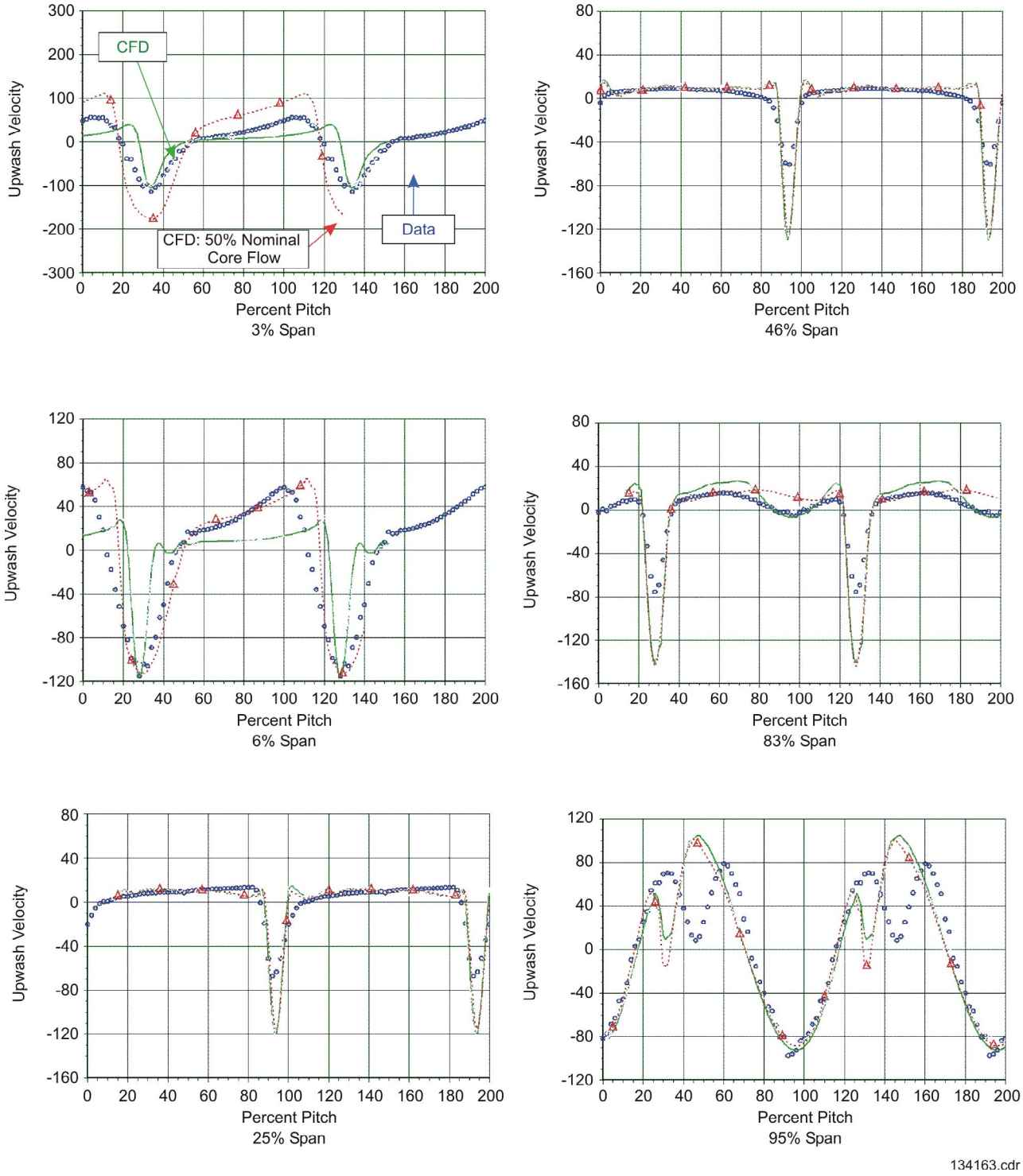

Figure 2-16. *Wake Comparisons at Station 1 of the ADP 22-in. Fan 1 with 50 Percent Core Flow*

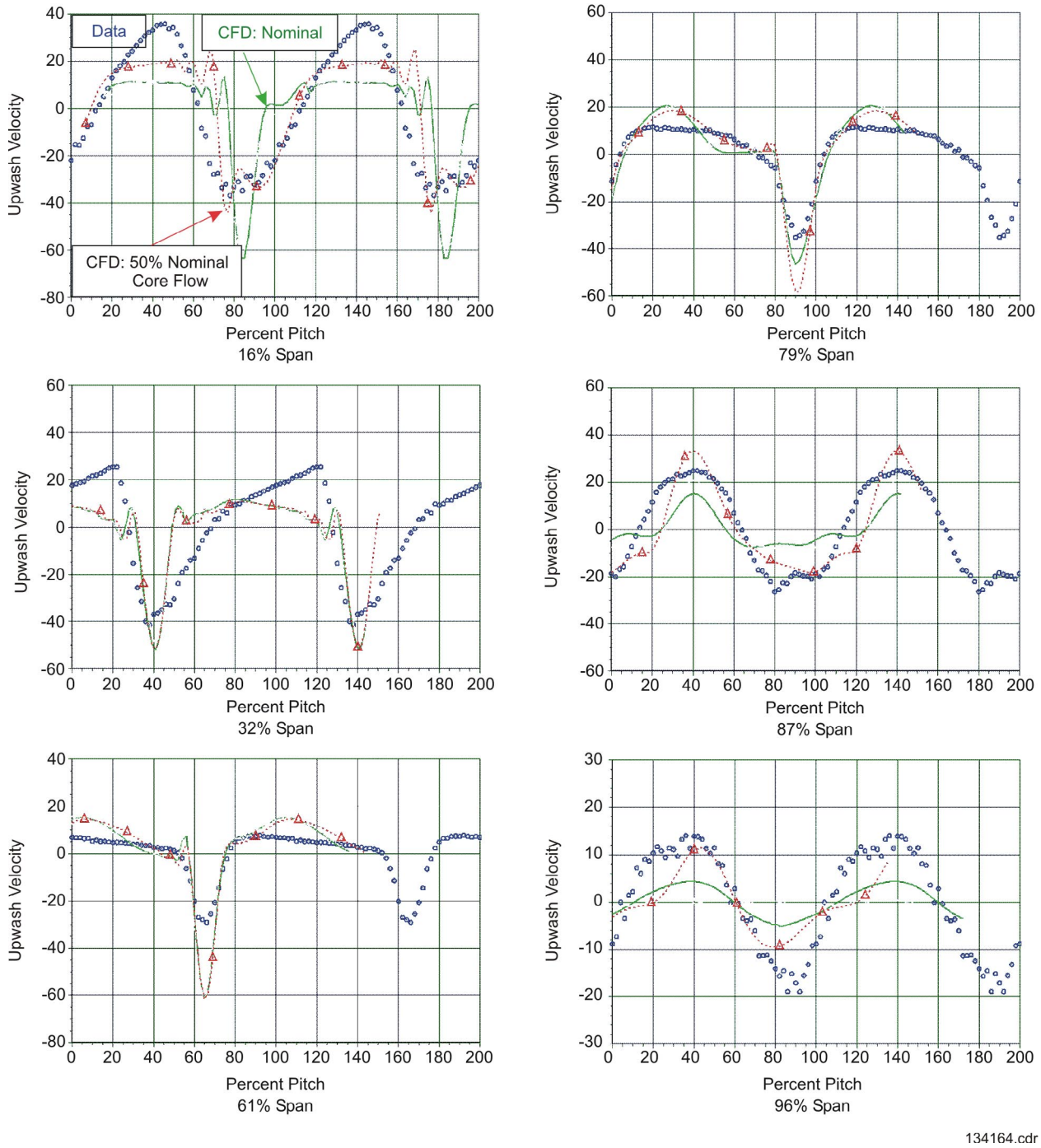

Figure 2-17. *Wake Comparisons at Station 2 of the ADP 22-in. Fan 1 with 50 Percent Core Flow*

2.1.5 CFD Model Conclusions

A noise prediction system is in place and integrated with CFD modeling. The CFD tool predictability has been assessed to gain understanding of fan noise sources, such as wakes and turbulence. The resulting tool predicts 3-D flowfield features well, from the blade trailing edge to about a chord downstream. However, the CFD tool loses accuracy as the distance from the trailing edge increases beyond a blade chord. In addition, the comparisons of CFD model predictions to data hinge on several assumptions. These assumptions encompass any modeled geometric discrepancies with actual geometry, the modeled inlet turbulence profiles, modeled turbulence transition, and the modeled fan/core flow split with test.

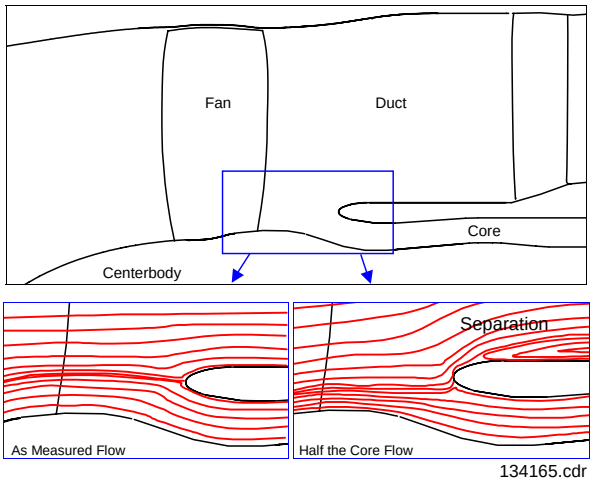

Figure 2-18. *Schematic of the Formation of a Flow Separation By Halving the Core Flow*

2.2 COMPARISONS OF NOISE PREDICTIONS TO RIG TEST DATA

The latest fan noise design capabilities were to be used to perform a preliminary fan stage design under this contract. The purpose of this section is to detail the fan design system and to validate this system with noise data. The preliminary fan stage design is discussed in Section 2.4.

2.2.1 Fan Noise Design System

The fan noise design system is shown in ***Figure 2-19***. As is shown, fan noise is separated into tones and broadband. Both the TFaNS (References 4 to 7) and the broadband-noise model (Reference 8 to 10) were developed under NASA funding. The input to these codes includes the fan and FEGV geometry and performance. Performance from a streamline curvature code and a Reynolds number-averaged Navier-Stokes code or from wake/turbulence test data may be used as input. The tone- and broadband-noise codes will now be described in further detail.

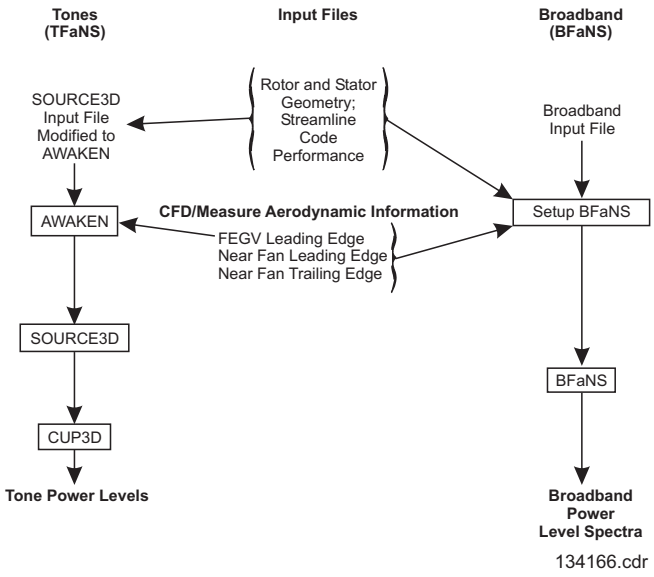

Figure 2-19. *Fan Noise Design Prediction System*

The TFaNS contains three major codes to produce fan tone noise predictions (***Figure 2-19***):

- *AWAKEN CFD/Measured Wake Postprocessor* creates a SOURCE3D input file that contains upwash wake harmonic amplitudes calculated from CFD predictions or measured velocity data. A modified SOURCE3D file (Reference 5) is used as input. In addition, CFD or measured velocity information is obtained from an Acoustic Wake/Turbulence File. This latter file is generated by either a CFD code (or postprocessor) or from the analysis of data from an engine/rig test program.
- *SOURCE3D Rotor/Wake Stator Interaction Code* (***Figure 2-20***) has two functions within the TFaNS: first, it calculates tone noise from a rotor wake/FEGV interaction, and second, it determines the scattering coefficients for the rotor and stator, and then outputs them to rotor and stator Acoustic Properties Files for use by CUP3D (see Reference 4). This code can either use its own internal semi-empirical wake model, or it can use CFD or measured wakes processed through the AWAKEN CFD/Measured Wake Postprocessor.

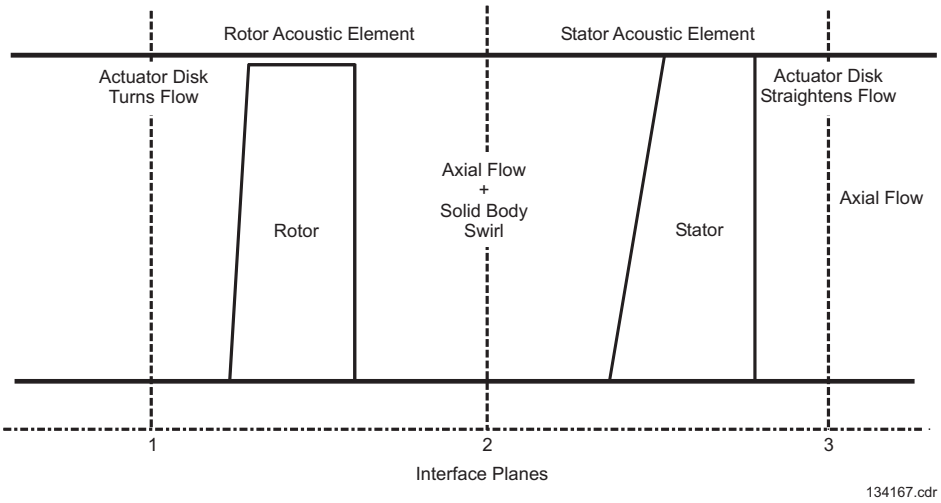

Figure 2-20. *TFaNS Tone Fan Noise Design/Prediction System*

All fan wakes and cascade unsteady pressures (on the fan or stator) are calculated or applied using a *strip* theory. Unsteady pressure distribution calculations are performed assuming flat plate cascades for each strip with a subsonic mean flow; hence, fans cannot be run supersonically. The noise calculation is completed by coupling the cascade unsteady pressures to acoustic modes that are assumed to be in a constant area annular duct with mean axial flow and solid body swirl (in between the fan and the FEGV). In addition, before the fan and aft of the stator are actuator disks that act to turn the flow, just as real blades and vanes would. This creates reflection and transmission effects in addition to those from the rotor and stator. The rotor and stator calculations are completed separately.

- *CUP3D Fan Noise Coupling Code* is the central portion of the TFaNS. The code reads Acoustic Properties Files that contain scattering (transmission and reflection) coefficients from SOURCE3D, as well as noise from the fan wake/stator interaction. This information is used to form a system of linear equations that permit the fan and the FEGV to reflect and transmit to each other. Output from this code includes inlet and aft power levels that are used during the design process.

For more information on these codes, see References 4 to 7.

The BFaNS has two major code calculations: The SetupBFaNS and the BFaNS (***Figure 2-21***). The SetupBFaNS obtains the geometry, performance, and flow turbulence from CFD predictions, streamline curvature code predictions, or measured data and organizes the BFaNS input file for the user. The BFaNS then uses this input file to predict noise sources shown in ***Figure 2-21.***

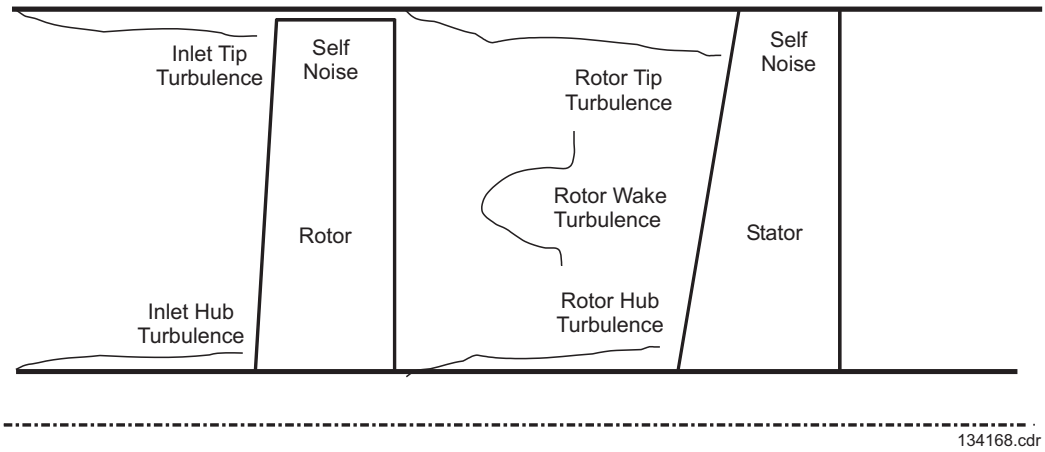

Figure 2-21. *BFaNS Fan Design Prediction System*

These noise sources include:

- Inlet tip and hub turbulence/rotor interaction (*blade tip* and *hub*, respectively)
- Rotor tip and hub turbulence/stator interaction (*vane tip* and *hub*, respectively)
- Rotor wake turbulence/stator interaction (*vane midspan*)
- Rotor and stator self noise (*blade* and *vane self*, respectively)

Each one of these noise sources is modeled separately. Details of this modeling may be found in References 8 to 10.

2.2.2 Evaluation of the TFaNS and BFaNS with Data

The ADP 22-in. Fan 1 rig data was used to validate the TFaNS and BFaNS capabilities. The ADP 22-in. rig acoustic and aerodynamic test data was obtained at the NASA GRC 9 ft × 15 ft low speed wind tunnel. The fan stage contains 18 blades and 45 vanes and runs at a top fan tip speed of 950 ft/sec. The rig includes a fan, an FEGV, and a core duct (***Figure 2-22***). Acoustic data was obtained with a microphone traverse at a constant sideline distance from the model and was postprocessed to a constant farfield radius from the rig. Tone and broadband noise was calculated by subtracting the broadband from the tone levels. Blade passing frequency (BPF) is cut off over the entire speed range in this rig. Reference 6 contains additional information on how this rig was configured for SOURCE3D.

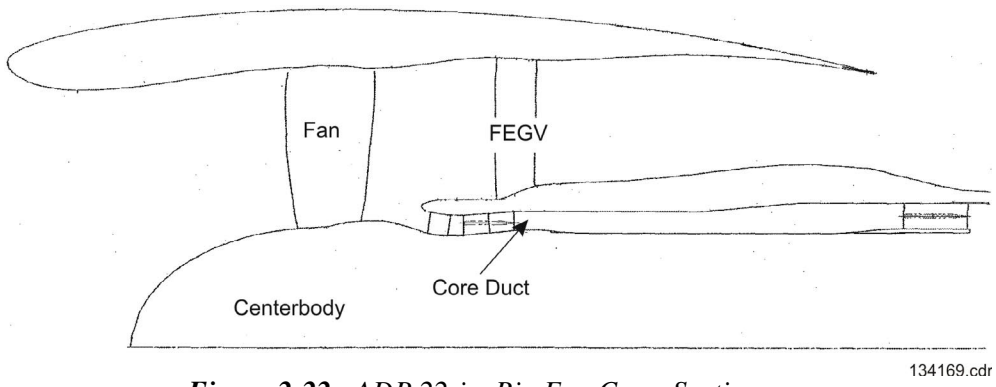

Figure 2-22. *ADP 22-in. Rig Fan Cross Section*

Verification of the system includes predictions using semi-empirical wakes (for the TFaNS only), experimentally measured wakes and turbulence (using hot wire/LDV), or CFD-predicted wakes and turbulence. Measurement stations for the experiment are shown in ***Figure 2-23***. As can be seen in this figure, in order to perform LDV and hot wire measurements, the FEGV was moved back. For the purposes of this study, the TFaNS predictions were based on flow data from Station 2 and the BFaNS predictions based on data from Station 1.

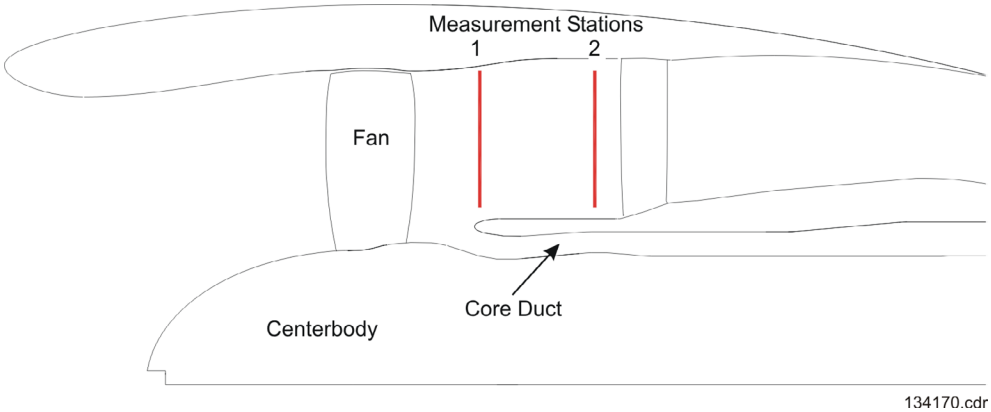

Figure 2-23. *ADP 22-in. Rig Fan LDV/Hot Wire Measurement Stations*

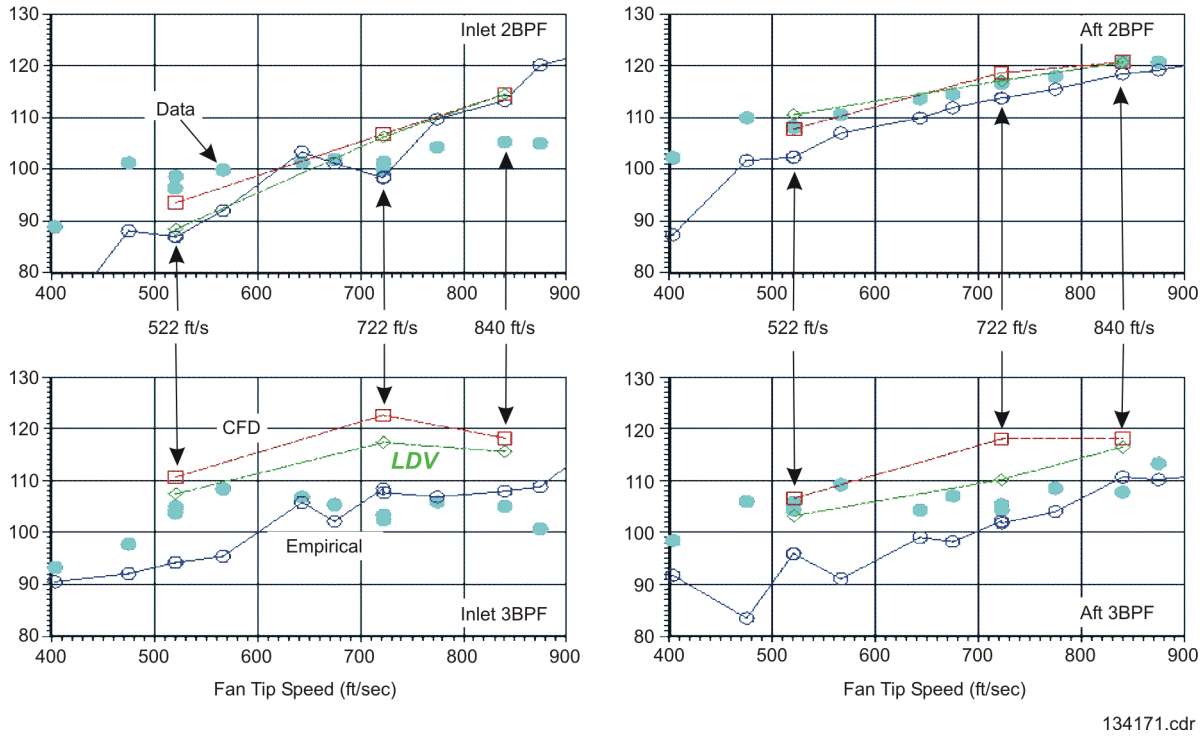

Figure 2-24. *ADP 22-in. Rig Fan 1 TFaNS Predictions Versus Data*

The TFaNS tone-noise predictions are presented in ***Figure 2-24***. Acoustic power level predictions were made using the code's semi-empirical wakes across the speed range. In addition, acoustic power levels were predicted with CFD-predicted wakes at the FEGV leading edge and LDV wake data from Station 2 (***Figure 2-23***). The two latter predictions were only made at the three speeds where the LDV data was obtained.

Results show that aft 2BPF data is well predicted using all prediction methods, but the best results are obtained from experimental or CFD wake data. Inlet 2BPF results vary, with prediction shapes not matching the data. Predicted levels match the data at different points along the operating line, depending upon the type of prediction. Inlet and aft 3BPF tend to be overpredicted by experimental and CFD wake data and are underpredicted by semi-empirical wakes below about 650 to 700 ft/sec. Semi-empirical predictions then appear to match the data above these tip speeds.

CFD wakes are shown against experimental wakes in Section 2.3.1 in ***Figures 2-12*** through ***2-15***. These wakes were employed at the FEGV leading edge to predict the noise above. The trailing edge of the stator is near the Station 2 measurement location (***Figures 2-22*** and ***2-23***) so that the FEGV leading edge is in between the two stations. ***Figures 2-12*** and ***2-13*** show that the wake phasing of the upwash velocity, used to calculate noise, is relatively well predicted by the CFD code at both Station 1 and Station 2.

Figures 2-14 and ***2-15*** show the tangential CFD wake upwash predictions versus data at various spans for the two flow measurement stations. A comparison of CFD predictions versus data at the FEGV leading edge is not available. However, noise predictions for the CFD wakes versus the LDV wakes at Station 2 predictions indicate that there is more 3BPF content in the CFD wakes than the measured wakes. This makes sense since the Station 2 CFD predictions versus experimental data show the CFD wakes to be thinner. Section 2.3.1 discusses the details of these predictions.

Overall, predictions tend to demonstrate reasonable agreement with data permitting the TFaNS to be used for design.

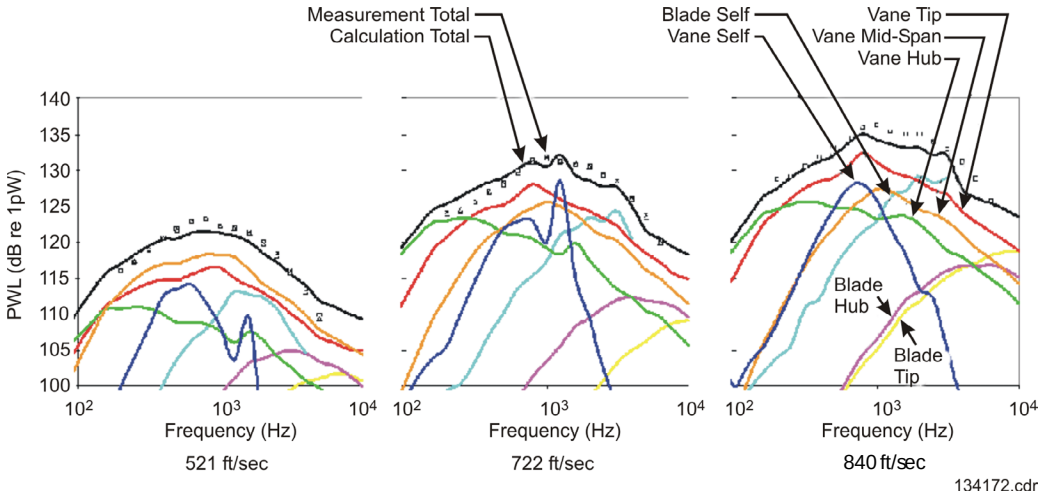

Figure 2-25. *ADP 22-in. Rig Fan 1 BFaNS Predictions Versus Data*

Broadband total power level noise predictions using the BFaNS are shown in ***Figure 2-25***. Data is represented by symbols, whereas predictions are represented by lines. The top black line is the calculated total power level predictions. The other lines show the predictions for the various noise sources. Predictions here are shown for the three operating tip speeds where LDV data was measured. LDV turbulence and fan performance information is used for these predictions at Station 1 **(*Figure 2-23*)**.

Predictions show good overall agreement with data. The predicted importance of a number of noise sources indicates the complicated nature of broadband noise. Vane generated noise sources, combined with fan self noise, appear to be significant. Fan tip turbulence interaction with the FEGV appears to produce the most important noise source for this rig at the two highest powers. This will become an issue in the stator design process in Section 2.4.2.

Figure 2-26 shows the circumferentially-averaged CFD-predicted fan-generated turbulence for ADP 22-in. rig Fan 1 at sideline power versus hot wire and LDV data at measurement Station 1. Results further reinforce the predicted importance of the fan tip turbulence and FEGV interaction. They also show that CFD models can predict the correct trends in circumferentially averaged noise, though the levels are underpredicted.

The above predictions for both tones and broadband show the importance of wakes and turbulence generated by the fan.

Overall, predictions tend to demonstrate reasonable agreement with data and permit the BFaNS to be used for design.

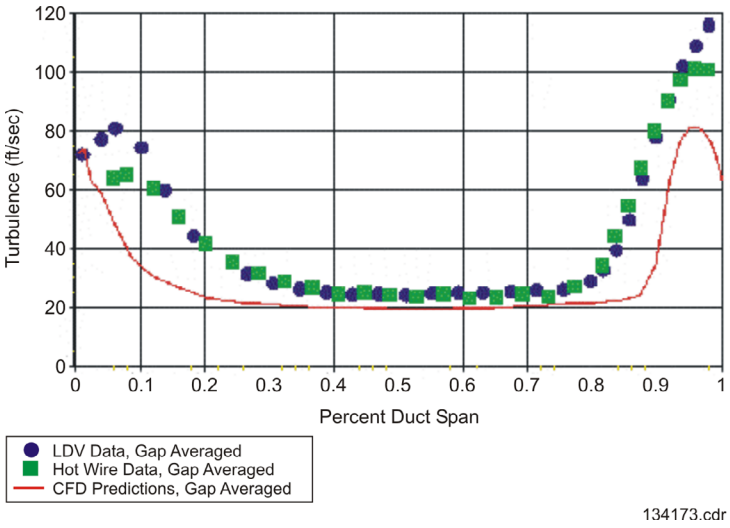

Figure 2-26. *ADP 22-in. Rig Fan 1 CFD Circumferentially-Averaged Turbulence Predictions Versus Hot Wire and LDV Data at Sideline Power at Measurement Station 1*

2.2.3 Analysis of Noise Differences between Fan 1 and Fan 2 Test Data

Along with the validation above, data from the ADP 22-in. rig was analyzed to determine the noise differences between two tested fans: Fan 1 and Fan 2. These fans are designed to run on the same operating line, but Fan 2's sideline tip speed is designed to be 10 percent lower than that of Fan 1. This reduced tip speed was expected to reduce noise further beyond that already achieved with Fan 1.

Effective perceived noise levels (EPNLs) for this effort were calculated using the standard aircraft flight path and takeoff gross weight (TOGW) (*e.g.*, 850,000 lb TOGW with 56,000 lb thrust engines) for NASA's AST program. Based on previous work, Fan 1 and Fan 2 were scaled to a 130-in. diameter fan.

Both fans have 18 fan blades and a 22-in. diameter. Fan 1 has 45 FEGVs while Fan 2 has 51 FEGVs, designed for low noise. The fan tip speeds at the various noise operating conditions are shown in ***Table 2-1.***

Table 2-1. *Fan Design Tip Speeds*[1]

Operating Condition	*Fan 1*	*Fan 2*
Approach (APP)	480 ft/sec	425 ft/sec
Cutback (C/B)	743	667
Sideline (S/L)	840	756

[1] See Reference 11.

Table 2-2 and ***Table 2-3*** show a summary of the results. ***Table 2-2*** indicates that, based on the standard 50 log (tip speed) scaling factor, fan tip speed reductions should reduce Fan 2 noise by 2.5dB relative to Fan 1. In addition, a 0.4dB increase is expected in the broadband noise due to the empirical 7 log (vane number) scaling factor from Boeing rig testing. Thus, a 2dB broadband noise reduction was expected.

Table 2-3 illustrates what was actually observed from the data when Fan 1 and Fan 2 were compared. The engines were *flown* with:

- Broadband noise data alone
- Total fan noise data.

As flown, results show a net broadband noise increase of about 1dB for Fan 2, relative to Fan 1. In addition, except at approach power, total fan noise increased by over 1dB.

Table 2-2. *Expected Results from Fan 1 Versus Fan 2 Comparison*

Fan 2 Quieter By:	*Reason*	*Empirical Basis*
2.5 dB	Lower fan tip speed	50 log (tip speed)
-0.4 dB (broadband only)	Higher vane number	Boeing tests: 7 log (vane number)
~2.0 dB	Net expected broadband noise reduction	

Table 2-3. *Observed Results from Fan 1 Versus Fan 2 Comparison*

Fan 2 Noisier By:	*Condition*	*Major Observations*
~(-0.1) EPNdB	APP	Fan 1 aft 2BPF higher (Fan 2 2BPF cutoff, Fan 1 2BPF cuton) Fan 2 broadband higher by 1.0 EPNdB
~1.4 EPNdB	C/B	Fan 2 broadband higher by 1.1 EPNdB
~1.7 EPNdB	S/L	Bandshared 2BPF in Fan 1 Fan 2 broadband higher by 0.9 EPNdB

Since these EPNL results indicate that broadband noise is the dominant noise source in the data, the BFaNS was used to evaluate this noise problem. ***Figure 2-27*** shows scaled (to 130-in. diameter fan) Fan 2 minus Fan 1 BFaNS predictions for the total broadband power levels at sideline power. The low frequency 1/3 octave bands (50 Hz to 125 Hz) were excluded because they are normally not fan noise dominated. The other 1/3 octave bands (8kHz and 10kHz) were excluded because no scaled data exists at these frequencies. Fan 2 data does in fact appear to be about 1dB higher than the Fan 1 data, which is consistent with the broadband EPNL calculations (***Table 2-3***). The BFaNS predictions also show an increase in noise on the order of 2dB. These consistent results show that the basic scaling rules used in ***Table 2-3*** do not apply to these two differently loaded fans.

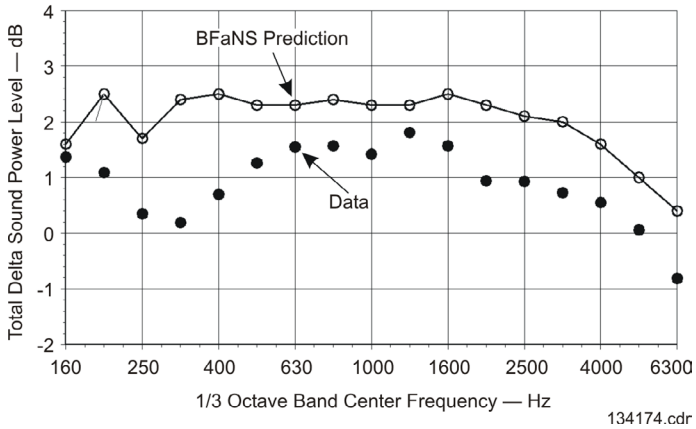

Figure 2-27. *Broadband Sound Power Level Deltas (Fan 2 Minus Fan 1) with 1/3 Octave Band Spectrum and Sideline Power*

Further examination of the BFaNS predictions finds that fan tip turbulence interaction with the FEGV was the major contributor to fan broadband noise. This noise rose in Fan 2 relative to Fan 1. ***Figure 2-28*** shows CFD predictions at the FEGV leading edge. These predictions illustrate the circumferential and radial content of the fan turbulence. Results show the rise in turbulence for Fan 2 relative to Fan 1. The cause of this increased turbulence is unknown.

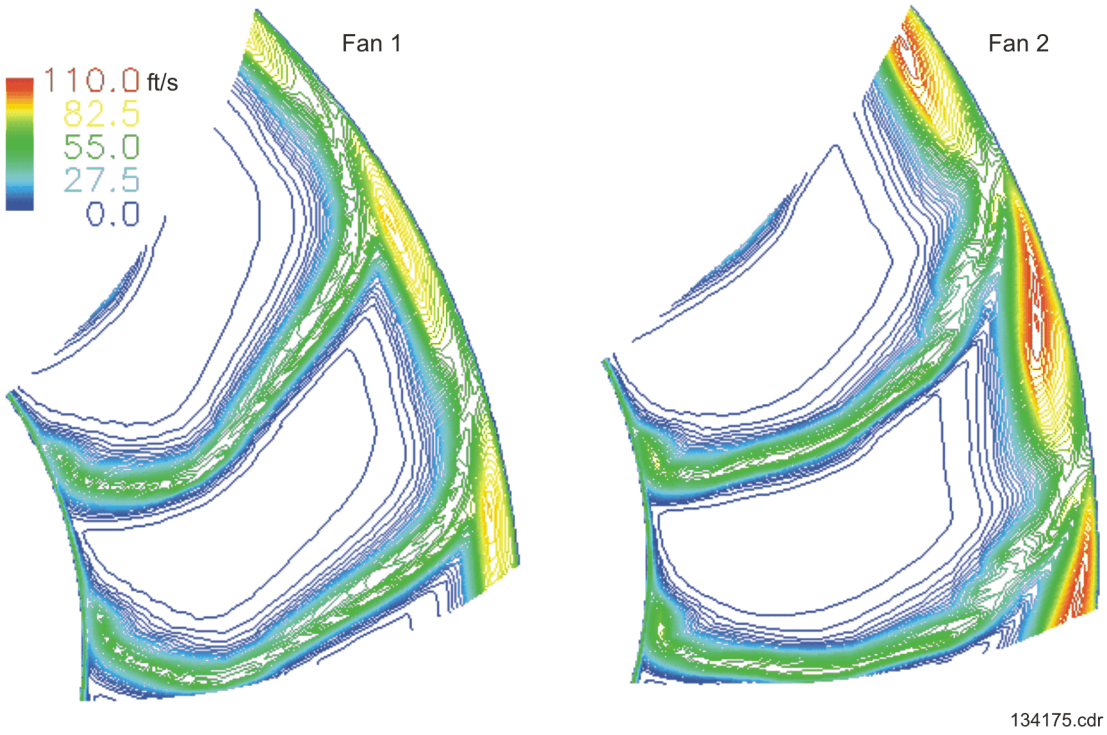

Figure 2-28. *Rotor Wake Turbulence at FEGV Leading Edge: CFD Prediction at Sideline Power*

At approach power, a small decrease in total fan EPNL is noted (***Table 2-3***). This decrease appears to be mostly because the 2BPF tone emanating from Fan 2 is cutoff, while it is cuton in Fan 1. Thus, at approach power, the total fan EPNL delta is strictly a vane number effect.

One other method was also employed to evaluate these Fan 1 versus Fan 2 results. As a result of work done by D.C. Mathews, a simple broadband sound power level formulation was developed. This formulation used the knowledge of basic isolated airfoil acoustics to determine possible scaling parameters for broadband noise. The formulation was then applied to sideline power. The D.C. Mathews formulation equation is:

$$Sound\ Power \propto 10\log\left[C^3 V_0^2 N_V\right]$$

Where:

- C = Absolute velocity into the stator (ft/sec)
- V_0 = Turbulence (ft/sec)
- N_V = Number of FEGVs.

Table 2-4 illustrates the results of this equation (given as the *P&W Results*) along with the results from the BFaNS and from data for broadband noise only. In all three cases, Fan 2 noise goes up rather than down, as conventional scaling factors might predict.

Table 2-4. *Results of Fan Broadband Noise Predictions Versus EPNL Calculations Using Data*

			Broadband Noise Delta (dB) (Fan 2 to Fan 1)		
Parameters Near Stator Tip Leading Edge (from CFD)	***Fan 1***	***Fan 2***	***P&W***	***BFaNS***	***Data***
Number of Vanes, N_V	45	51	0.5		
Absolute Velocity, C (ft/s)	594.3	630.1	0.8		
Turbulence, V_o (ft/s)	73.1	82.7	1.1		
Total Broadband Delta (dB)			2.4	~2.0	~0.9

Thus, in conclusion, the goal of Fan 1 was to reduce fan tip speed while increasing fan loading. Fan 2 was intended to go further with this concept. However, it was apparently too highly loaded to support a further decrease in tip speed.

In Section 2.4, a preliminary fan and FEGV design are shown, which were intended for the next build of this rig (that was dropped from the contract).[1] The fan design in Section 2.4.1.2 uses Fan 2 as a baseline for improvements. The FEGV design in Section 2.4.2 features Fan 1 as its baseline fan and details the creation of a new design from this fan stage.

2.3 RIG AIRFLOW AND INLET SEPARATION ANALYSIS

This section describes the method used to determine the total fan airflow used in the analysis and includes comparisons of measured boundary layer profiles to predictions for verifying rig airflows. In addition, it describes the analysis used to determine the inlet separation angle-of-attack and shows a typical inlet distortion pattern that was produced during angle-of-attack/fan surge margin distortion testing. This discussion is split up into three sections. The first section, Section 2.3.1 describes the inlet configuration and instrumentation. Section 2.3.2 describes the method to determine airflow, and Section 2.3.3 covers inlet distortion and separation angle-of-attack.

[1] The next rig build was dropped from the contract.

2.3.1 Inlet Configuration and Instrumentation

The 22-in. rig inlet configuration (shown in ***Figure 2-29***) used in this test was designed:

- With an inlet throat area (A_t) that is sized for a maximum corrected flow of 99.53 lb/s without an internal shock.
- To have a shock free external contour.
- To be separation-free up to a 27-degree angle-of-attack at a takeoff corrected airflow of 90 lb/s.

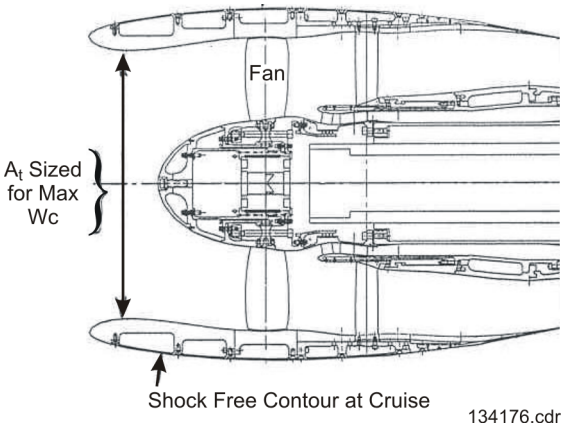

Figure 2-29. *ADP 22-in. Rig Inlet*

Figure 2-30 shows the 22-in. rig inlet instrumentation. During rig performance testing, the inlet wall static pressures at Station 2 were used to obtain total fan airflow, while the axial static pressures and the total pressure boundary layer probes/pole rakes were used to measure inlet separation and distortion. The boundary layer probes were also be used to verify the predicted boundary layer thickness used in the airflow calculation.

2.3.2 Method to Determine Fan Airflow

Airflow is determined from the method shown in ***Figures 2-31*** and ***2-32***, where a code calibration process and measured wall pressure was used. To describe this in more detail, a correlation between measured static pressure and inviscid airflow was created in a parametric inviscid CFD study of the inlet. The airflow was then adjusted for viscous effects by calculating a ΔC_D correlation through the use of a standalone strip integral boundary-layer code. The information from these two calculations was combined to create a correlation between measured Station 2 static pressure and corrected airflow

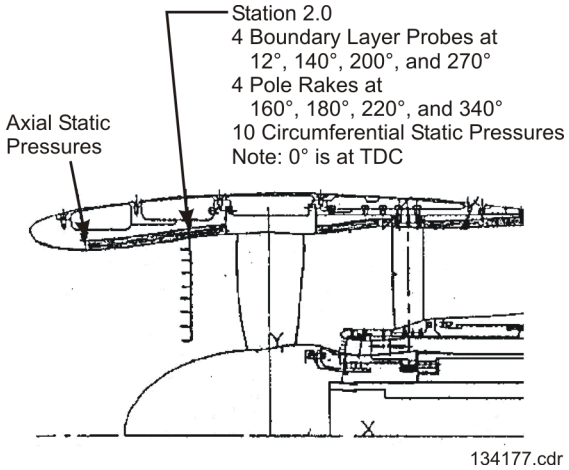

Figure 2-30. *Description of the 22-in. Rig Inlet Measurements*

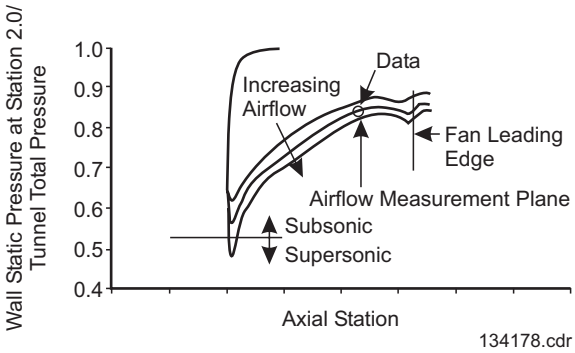

Figure 2-31. *Wall Static Pressure Versus Axial Distance for Several Airflows*

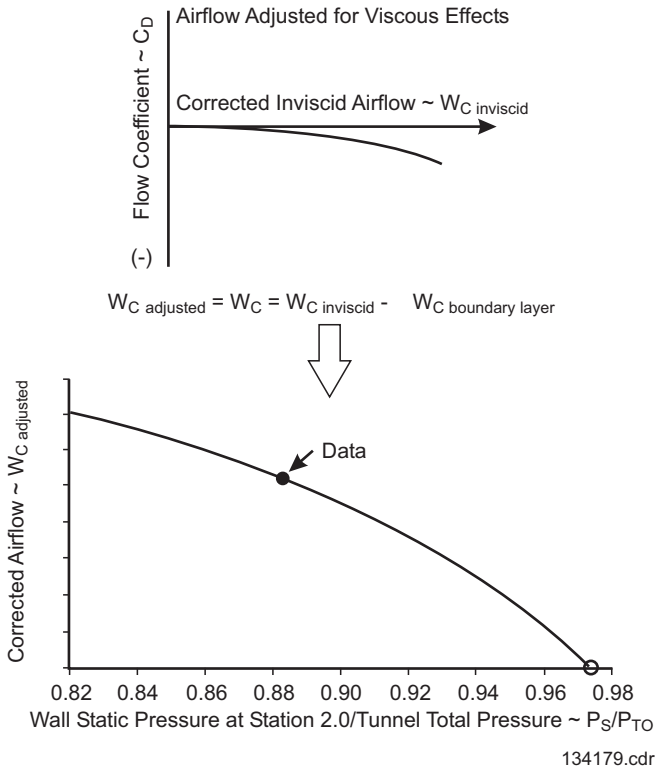

Figure 2-32. *Airflow Adjusted for Viscous Effects and Correlated with P_S/P_{TO}*

In order to check the accuracy of the boundary-layer calculation used to account for the viscous effects in the airflow prediction method, output parameters (shape factor, boundary-layer thickness and edge Mach number) from a standalone strip integral boundary-layer calculation were used to calculate the predicted boundary layer total pressure profile. The calculation was then compared to measured data. This comparison can be seen in ***Figure 2-33*** where predicted total pressure profile (lines) for two airflows (80.54 lb/sec and 57.7 lb/sec) are compared to data (symbols). Except near the edge of the profile, the prediction agrees well with the data.

2.3.3 Inlet Distortion and Separation Angle of Attack

The inlet separation angle was determined by monitoring the static and total pressure instrumentation on the model. ***Figure 2-34*** shows how the instrumentation was used. The first figure shows that before the onset of inlet separation, at a given angle-of-attack, the high rate of flow curvature around the inlet lip produces minimum pressure measurements that result in peak values of surface Mach numbers (low-static pressure). As inlet angle-of-attack is increased, lip separation begins to occur, producing a local separation bubble. This separation bubble causes a reduced rate of curvature and results in lower levels of peak Mach numbers. As the angle-of-attack is increased, the separation region grows until there is very little or no lip suction. In addition, the inlet separation produces a total pressure deficit in the separated region. The second figure shows the distortion parameter that is a measure of the total pressure loss. The inlet distortion in front of the fan is shown in the last figure. It should be noted that the surface pressures around the lip provide a reliable indication of the inlet separation and, as such, were used as the primary indicator of separation.

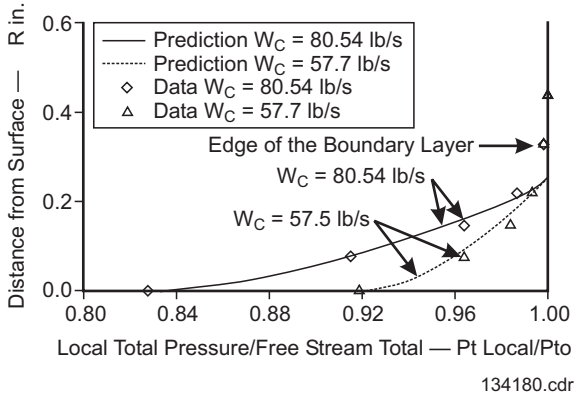

Figure 2-33. *Comparison of Boundary Layer Total Pressure Profile Prediction Versus Data*

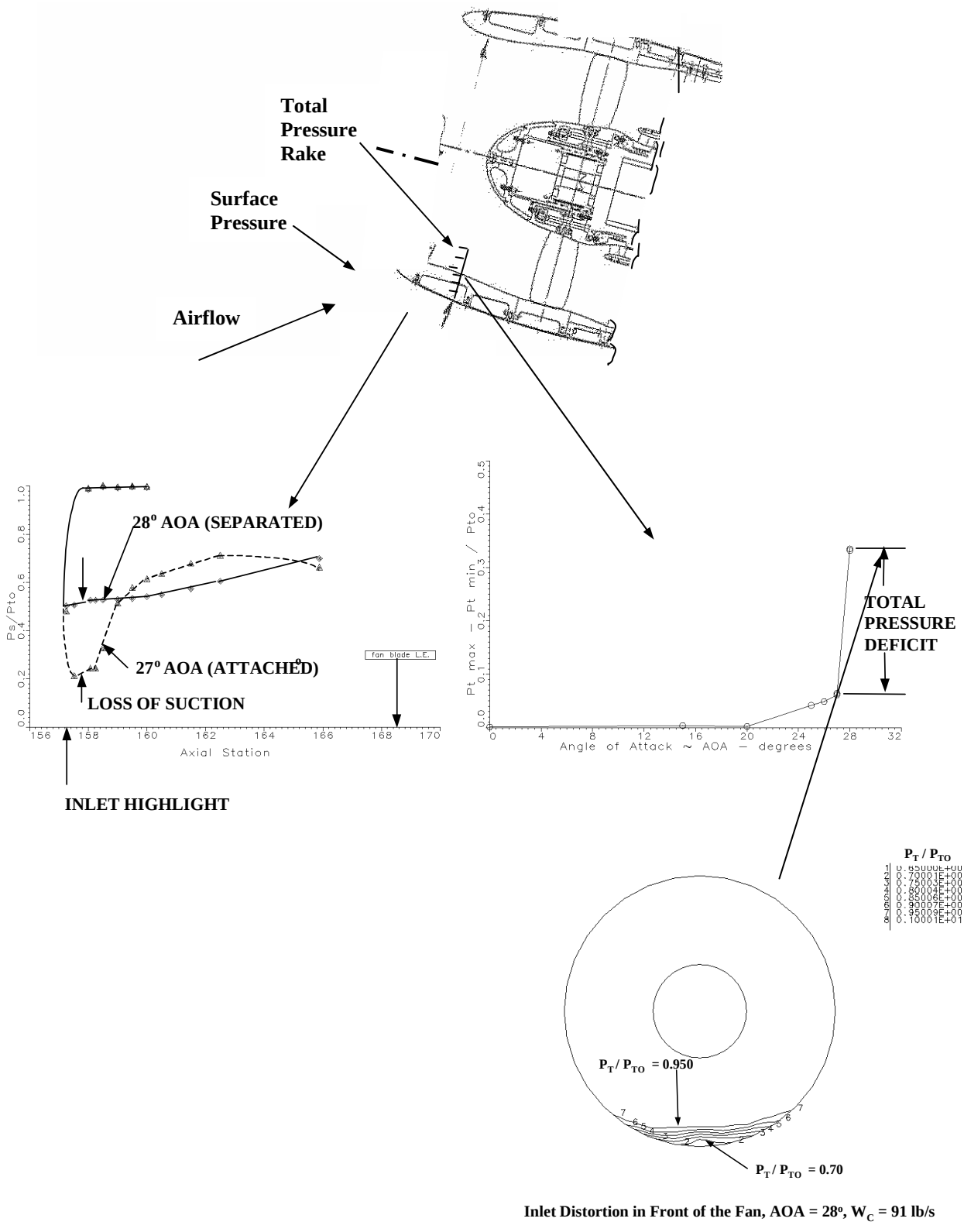

Figure 2-34. *Typical Change in Pressure When Separation Occurs (Configuration 62; Mn=0.2; W_C=91 lb/s)*

Using these indicators to determine inlet separation, the 22-in. rig separation angle-of-attack was determined for a range of tested airflows and is depicted in ***Figure 2-35***. As indicated, above the line the inlet flow is separated, while below the line it is attached.

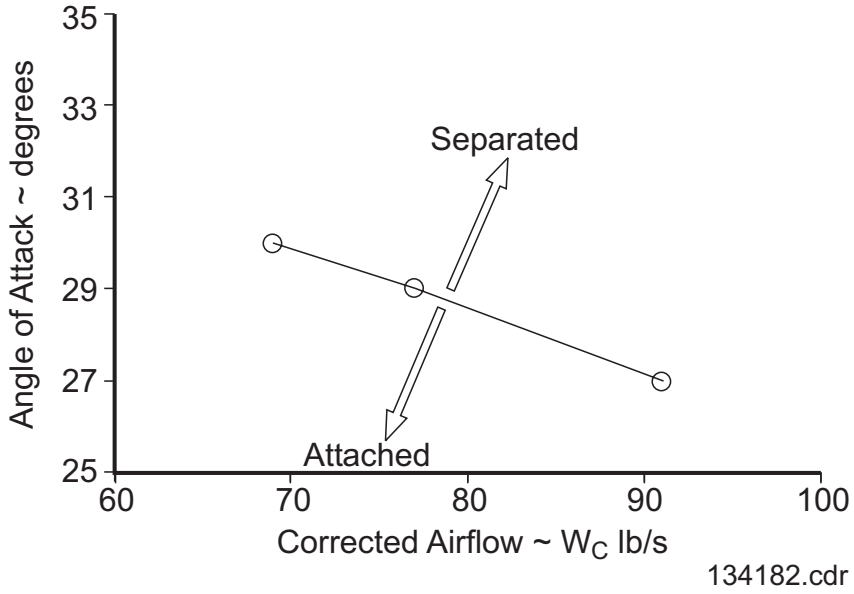

Figure 2-35. *Inlet Angle-of-Attack Versus Corrected Airflow*

3. FAN DESIGN OPTIMIZATION STUDIES

3.1 ROTOR PARAMETRIC STUDIES

In support of the reduced noise goals for Fan 3, parametric studies were conducted on the rotor to investigate the effects of fan loading distribution on fan noise. Fan 2 was used as the baseline fan stage for this study.

To perform the studies, general design concepts were considered jointly by aerodynamic and acoustic designers. An aerodynamic designer proposed designs that were reviewed with an acoustic designer. The acoustic designer then predicted the noise for each design using the CFD wake and turbulence information produced by the aerodynamicist as input to the fan noise design system outlined in ***Figure 2-19***.

3.1.1 Aerodynamic Configurations

The following aerodynamic configurations were considered for acoustic evaluation:

- *ADP 22-in. rig Fan 2* – baseline
- *ID-biased fan loading* – fan loading is biased towards the hub of the fan, *i.e.*, the hub is doing more work to turn the flow. ***Figure 3-1*** illustrates the radial pressure profile variations relative to the baseline Fan 2 profile.
- *OD-biased fan loading* – fan loading is biased towards the tip of the fan, *i.e.*, the tip is doing more work to turn the flow (***Figure 3-1***).

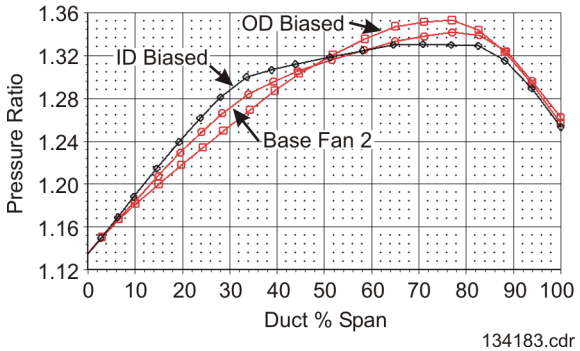

Figure 3-1. *Radial Profile Variation*

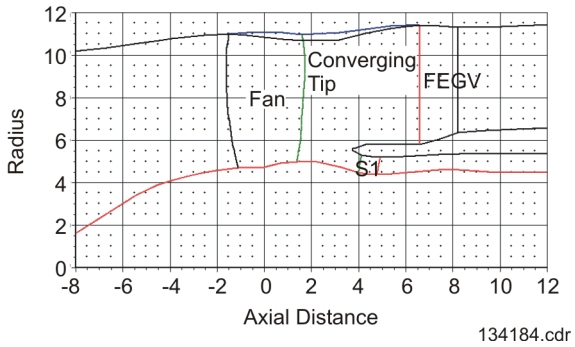

Figure 3-2. *Converging Tip Flowpath*

- *Converged fan tip* – the original flowpath has no convergence in the tip region; this was done so that the fan could have variable pitch capabilities. By converging the fan tip, it was anticipated that better fan performance would result. ***Figure 3-2*** shows the converged tip relative to the original flowpath.
- *Forward swept fan* – the effect on wakes was investigated when the fan was swept forward. This fan needed to be run at a different operating point (*e.g.*, flow and pressure ratio) than the other cases because of the sensitivity of this preliminary design. ***Figure 3-3*** illustrates the forward sweep and ***Figure 3-4*** shows the swept fan operating line change.

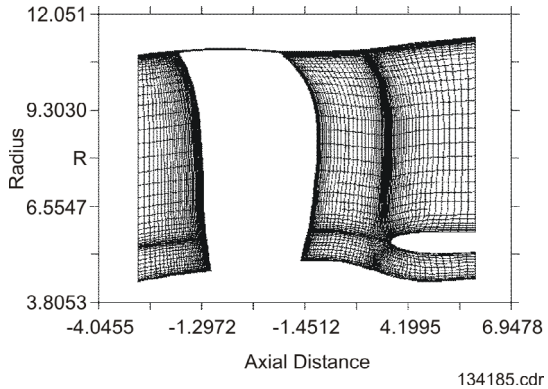

Figure 3-3. *Forward Swept Fan*

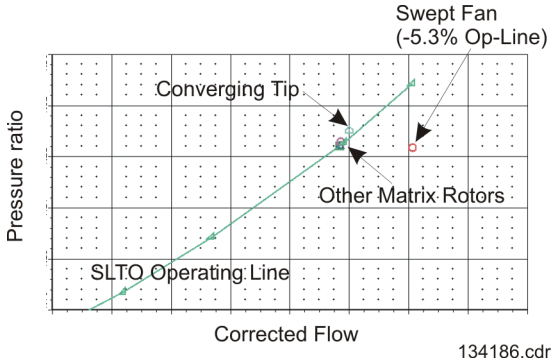

Figure 3-4. *Forward Swept Fan Operating Line*

- *Increased tip chord* – an increased tip chord configuration as shown in ***Figure 3-5*** was also considered. This case was not run for acoustics because there was so little change in the fan wake/turbulence quantities predicted by the CFD code.

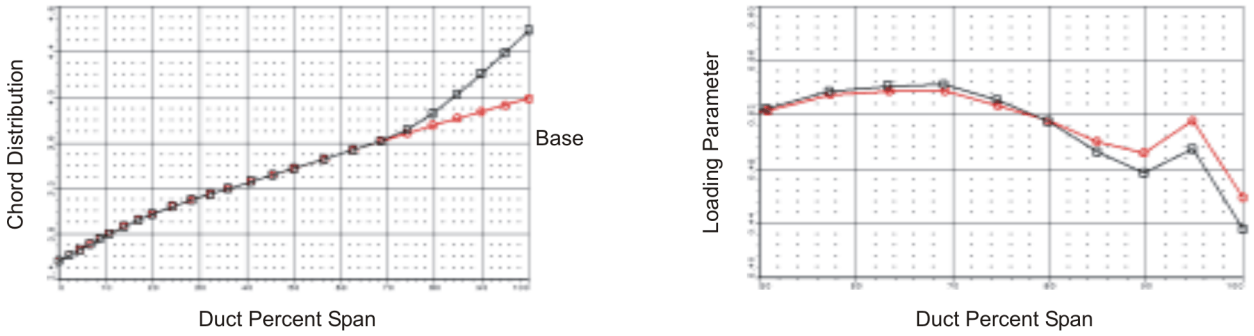

Figure 3-5. *Increased Tip Chord Distribution and Loading Parameter*

The output of the 3-D Navier-Stokes studies of the selected rotor configurations is predicted circumferentially-averaged turbulence and wakes. ***Figure 3-6*** shows the predicted turbulence for the various rotor configurations. ***Figure 3-7*** shows an expanded scale for the duct tip region.

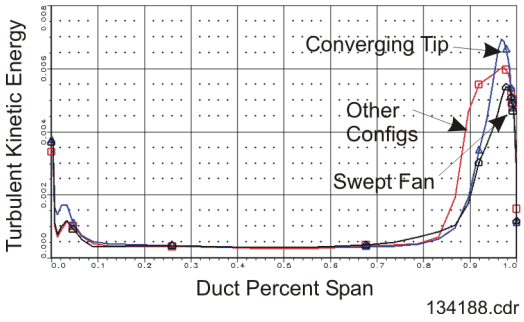

Figure 3-6. *Predicted Circumferentially-Averaged Turbulence*

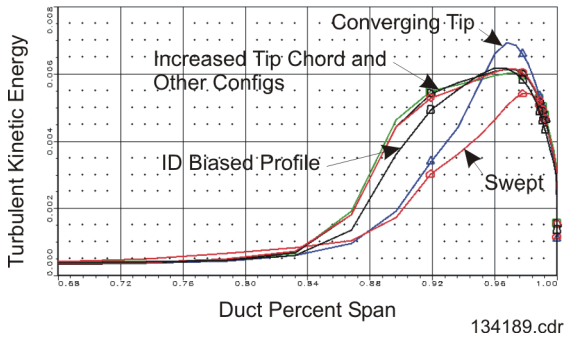

Figure 3-7. *Predicted Circumferentially-Averaged Turbulence – Tip Region*

Predicted wakes for the baseline (Fan 2) and ID- and OD-biased configurations are illustrated in ***Figure 3-8***; predicted wakes for the other configurations are depicted in ***Figure 3-9***.

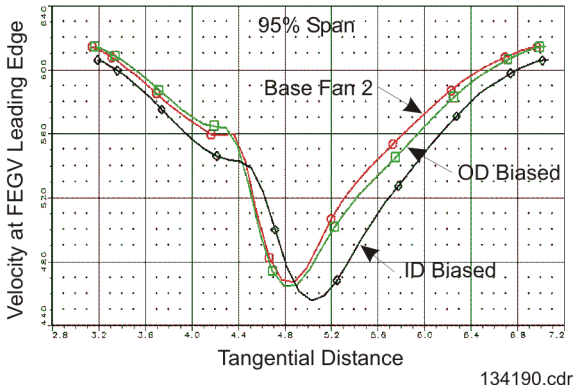

Figure 3-8. *Predicted Fan Wakes for Base Fan 3 and ID and OD Configurations*

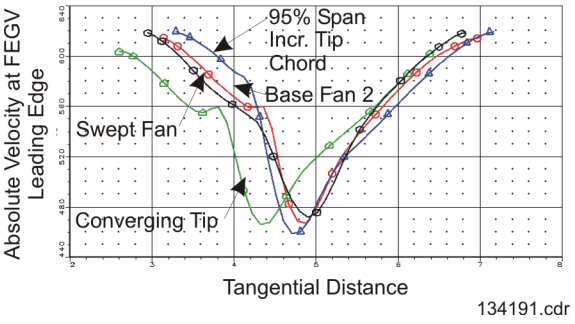

Figure 3-9. *Predicted Fan Wakes for All Other Configurations*

In conclusion, ***Figures 3-6*** and ***3-7*** show that turbulent kinetic energy for all configurations is similar out to the 85 percent span location. In the tip region, ***Figure 3-7*** shows that only the swept fan profile and the converging tip profile differ from the others, with the swept fan showing the lowest profile.

Figures 3-8 and ***3-9*** show general similarity for the wake profiles at the 95 percent span location.

The effect on acoustics for the turbulence and wake profiles illustrated previously is discussed in the next section.

3.1.2 Acoustic Studies

Section 3.1.1 discusses the configurations considered by the aerodynamic/acoustic team. For this design study, only the sideline operating condition was considered (756 ft/sec for Fan 2; see ***Table 2-1***). Tone noise predictions were made by coupling the rotor and stator, with a rotor wake/stator interaction noise source as the driver (***Figure 2-20***). All broadband noise sources were predicted according to ***Figure 2-21***. Delta power levels from the baseline Fan 2 design were determined and added to Fan 2 farfield acoustic data. EPNL predictions were then performed using the engine/aircraft configuration outlined in the beginning of Section 2.3.3.

Table 3-1 shows the tone noise deltas (relative to Fan 2 noise levels) for each tone, inlet, and aft. In this configuration, there are 18 blades, and 51 vanes making BPF cutoff. Results show that the best configuration for tones is for an ID-biased fan. However, the OD-biased fan also shows noise reductions.

Table 3-1. *Fan Tone Noise Predicted Deltas*[1]

	Inlet		***Aft***	
Configuration	***2BPF***	***3BPF***	***2BPF***	***3BPF***
Converged Tip	1.0	1.2	1.3	-2.5
ID Biased	-4.6	-5.4	-5.0	-6.8
OD Biased	-3.0	-1.5	-2.6	-6.3
Forward Swept	2.5	3.0	1.8	2.6

[1] Power levels relative to baseline Fan 2 and CFD wakes.

The forward swept fan blade configuration shows a noise increase, while the converged fan tip case causes only a modest noise increase. The forward swept fan was likely impacted by the subsonic nature of this fan's tip speeds, combined with the preliminary design issues associated with the fan.

The reason for the fan tone noise reductions with the ID-biased fan appears to relate to the interaction of the rotor wake phasing with the FEGV. This interaction is seen in ***Figure 3-10***, which shows the upwash velocities for the two fans (*i.e.*, the flow variation through the wake, perpendicular to the mean absolute velocity into the FEGVs). Since the FEGV leading edge is a radial line from the rig centerline, more of the wake is radial and *slapping* the FEGV with the baseline Fan 2 than with the ID-biased loaded fan. This effect appears to be important to the noise; it causes a noise reduction for the ID-biased loaded fan. Also in ***Figure 3-10***, the wakes appear to not be smooth. This results from how the wakes are interpolated by the plotting routine used for this visualization and does not impact the noise source.

In further analysis, it appears that the wake harmonic magnitudes at the FEGV leading edge do not vary much. ***Figure 3-11*** illustrates this point by showing the ID-biased wake harmonic magnitudes of 20 log (wake harmonic magnitude) versus those of the baseline Fan 2 calculation. Based on noise theory, the 20-log calculation denotes noise differences at the various harmonics. There is little difference between the two fans for 2BPF and 3BPF, indicating that the wake phase interaction with the stator geometry explains the great majority of the difference between the two fan tone noise levels. Similar results are found for the other fans.

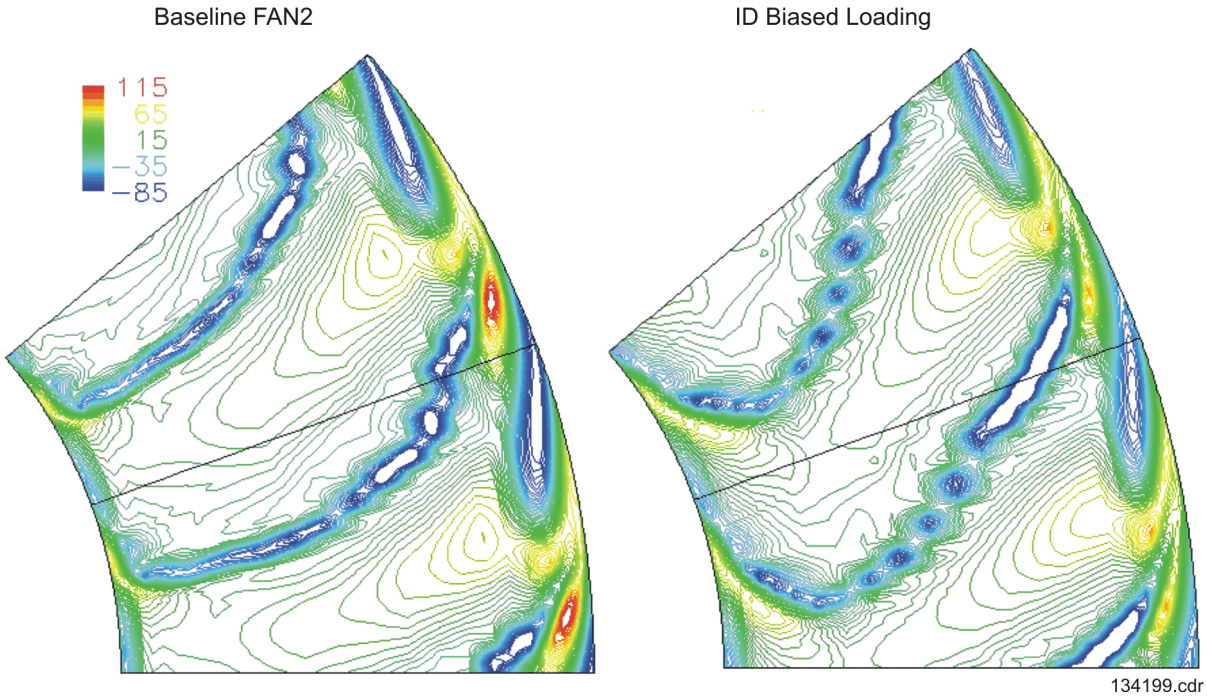

Figure 3-10. *Wake CFD Predictions Near FEGV (Upwash Velocity [ft/sec])*

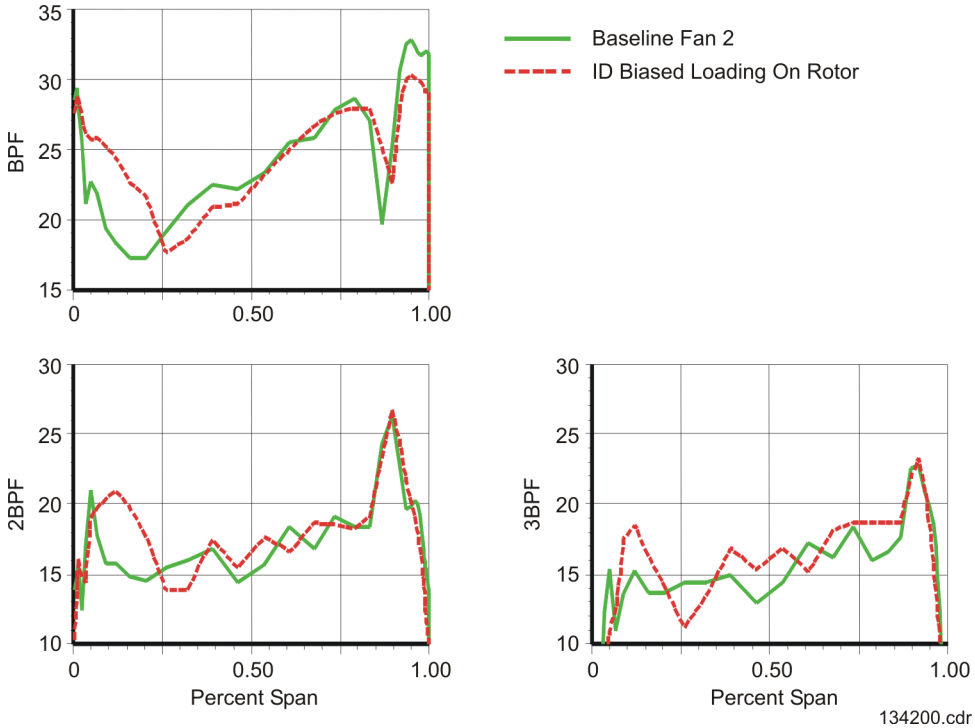

Figure 3-11. *Fourier Decomposition of CFD Wake Upwash (20 Log [Wake Harmonic Magnitude])*

Thus, the following conclusions are made about the tone noise predictions for these various fan designs:

- The ID-biased loaded rotor is the quietest
- Wake harmonic magnitudes are similar for the different rotors
- Predicted tone noise changes appear to be largely due to rotor wake phase lag.

Figure 3-12 shows the broadband noise deltas (relative to the Fan 2 noise levels) for the ADP rig, scaled to a 130-in. diameter fan, inlet, and aft. Broadband levels are given on a narrowband basis. Results are color coded in order from highest to lowest noise levels:

- Converged tip is red
- Forward swept is blue
- OD biased is orange
- ID-biased is green.

Results show very modest noise reductions for the ID-biased fan and near zero noise reductions for the OD-biased fan. Other fans show a noise increase.

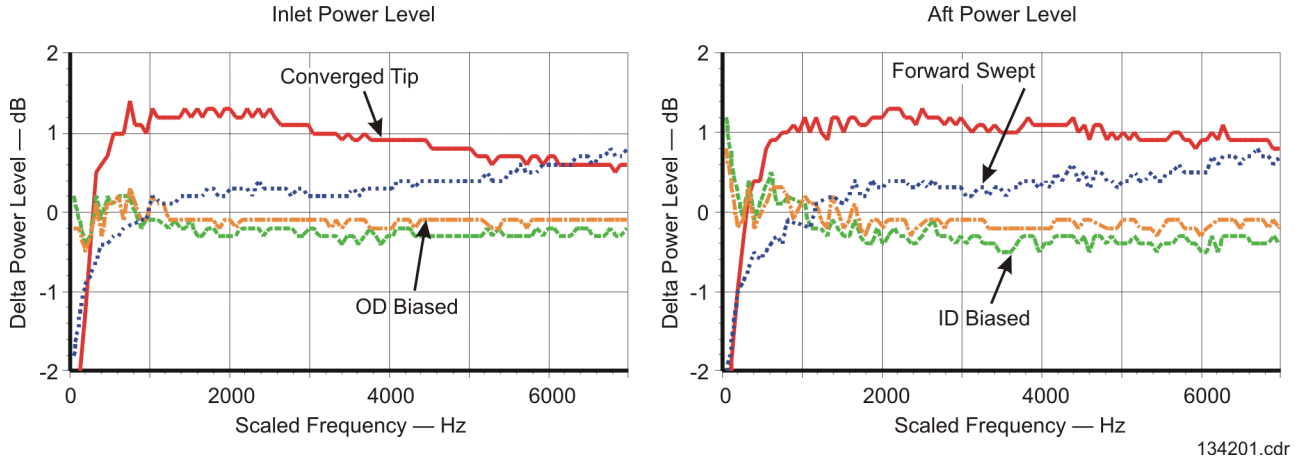

Figure 3-12. *Fan Broadband Predicted Deltas Scaled to 130-in. Diameter Fan (Delta Power Levels Relative to Baseline Fan 2 and CFD Turbulence Used as Input)*

Overall, fan tip turbulence interaction with the stator is predicted to be the most important noise source for these fans. To investigate these results somewhat further, the predicted circumferentially-averaged turbulence intensities at the FEGV leading edge are shown for all fans in ***Figure 3-13***. These turbulence intensities, in part, determine the noise levels for the fan wake turbulence/stator interaction noise (for midspan turbulence), fan tip turbulence/stator interaction (tip turbulence), and fan hub turbulence/stator interaction (hub turbulence). There is little difference in the turbulence levels at the center of the FEGV. At the hub and the tip, there are some differences predicted by the CFD code. However, these differences are mainly confined to the converged tip and forward swept fan configurations. This explains the small changes seen in the OD-biased and ID-biased broadband noise levels relative to the baseline fan. Thus, broadband noise predictions show the following characteristics:

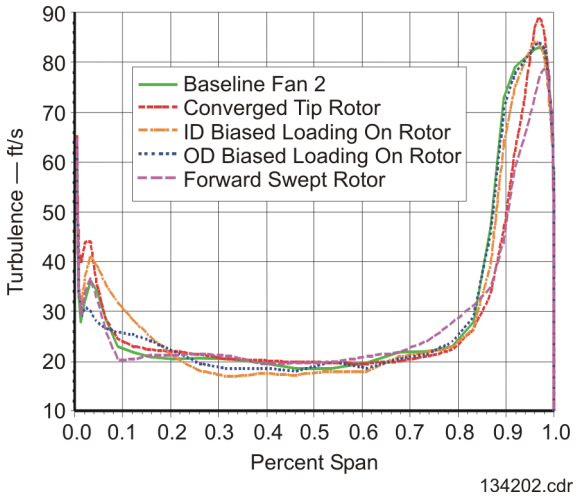

Figure 3-13. *CFD Predicted Circumferentially-Averaged Turbulence (ft/sec) Near FEGV Leading Edge*

- The ID-biased loaded rotor is the quietest
- Turbulence levels are similar for all fans
- Fan tip turbulence/stator interaction dominates at most frequencies
- Inlet boundary layer turbulence/rotor interaction dominates at very high frequencies.

To best understand these results, the tone- and broadband-predicted deltas (relative to Fan 2 predictions) are added to the Fan 1 and Fan 2 data and flown in the 130-in. diameter fan configuration engine at flight conditions. For the purposes of simplicity, only the results from the ID-biased fan, the best fan configuration, are shown in the form of deltas from the baseline ADP 22-in. fan rig configurations (***Table 3-2***).

EPNL predictions were completed using three different methods:

- Adjust for tones – database adjusted for tone deltas only (no broadband deltas added)
- Adjust for broadband minus 0.3 dB – database is adjusted down 0.3 dB for broadband noise only. This is the average noise reduction found in ***Figure 3-12***
- Adjust for tones and broadband – full EPNL prediction, including both tone and broadband noise.

Results of these EPNL predictions are shown in ***Table 3-2***. By adjusting for tones and broadband separately, the impact of each of these noise components on the total EPNL reduction is investigated. Also, predictions are shown using two different baseline configurations, Fans 1 and 2. This provides information on the impact of using either fan stage as a baseline, even though tone and broadband deltas are all relative to Fan 2.

As can be seen, the EPNL noise reductions observed are mainly due to the predicted reductions in fan tone noise. Broadband noise reductions were minimal.

Table 3-2. *Results of the EPNL Predictions*[1]

	EPNL, ΔEPNdB	
BASELINE	***Fan 2 (756 FPS)***	***Fan 1 (840 FPS)***
Adjust for Tones	-1.66	-1.40
Adjust for Broadband minus 0.3 dB	-0.14	-0.18
Adjust for Tones and Broadband	-1.89	-1.57

[1] 130-in. ADP large quad aircraft; sideline configuration; hardwall Fan 2 data; smooth rubstrip; ID-biased loaded fan relative to baseline Fan 2.

Thus, our results indicate that:

- Full-scale sideline noise predictions show that EPNL reductions are possible by changing the rotor design
  - — 0 to -2 EPNdB for lower tones
  - — 0 to -0.2 EPNdB for lower broadband
  - — 0 to -2 EPNdB for lower overall fan noise.
- Tone noise reductions appear to be due to wake phase lag changes, and not wake strength/width changes; consequently, equivalent tone noise reductions should be achievable through proper vane design.
- Broadband noise reduction changes are minimal or cause more noise.
- The baseline fan chosen (Fan 1 versus Fan 2) has little impact on these conclusions.

3.2 FEGV PARAMETRIC STUDIES

The results of the rotor parametric study (Section 2.4.1) indicated that broadband noise reduction was minimal and that tone noise reduction should be achievable through proper FEGV design. After presentation to NASA management and joint review of these results, agreement was reached to continue work on optimizing FEGV stator designs with the rotor design of Fan 1.

To perform the studies, general design concepts were considered by aerodynamic and acoustic designers. Based on these discussions, aerodynamic designers developed designs. Acoustic designers discussed the designs with aerodynamic designers and predicted the noise for each design using the fan noise design system outlined in a process, which will be discussed below. Fan 1 was used as the baseline fan stage for this study.

Table 3-3. *FEGV Parametric Study/Preliminary Design Matrix*

Parameter	*Level*	*Vane No.*	*Tone*	*Broadband*	*Leading Edge*	*Potential Benefit*
1) Baseline Fan 1 radial vanes in forward position	--	45	X	X	Forward	Baseline
2) Vane number (constant solidity)	--	11 to 79	X	X	Forward	Fewer vanes reduces broadband (cuton)
3) Solidity (chord change)	20% chord	11 to 79	Not run for noise		Forward	Needed for structural reasons
4) Stacking line variation (sweep)[1]	30 deg. sweep	11 to 79			Forward	Improves wake/vane phasing; decreases lift fluctuations
5) Stacking line variation (bow/lean)	--	11 to 79			Forward	Improves wake/vane phasing
6) Stacking line variation (bow/lean and sweep)	30 deg. sweep	11 to 79			Forward	Improves wake/vane phasing; decreases lift fluctuations
7) Baseline Fan 1 radial vanes in forward position with simulated tip boot	45 deg. in tip region only	11 to 79			Forward	Reduced broadband noise if dominated by fan tip turbulence/stator interaction

[1] With +20 percent aerodynamic chord.

The configurations shown in ***Table 3-3*** were considered for aerodynamic and acoustic evaluation. The configurations outlined below use the same numbering system as in ***Table 3-3***. ***Figures 3-14*** and ***3-15*** illustrate the general vane geometries that were predicted. The configurations are:

1) *ADP 22-in.Fan 1 rig FEGV* – Baseline.

2) *Vane number study with constant FEGV solidity* – These studies assumed the vane solidity (chord/pitch ratio) remained constant as the vane number changed. This assumption was used for all vane number studies of the configurations below.

3) *Solidity (chord change)* – This configuration involved adding 20 percent to the FEGV aerodynamic chord in preparation for sweep/lean/bow studies that may require the additional stiffness. This relatively modest chord change was not considered acoustically significant; thus, it was not predicted.

4-6) *Stacking line variations* – These variations included adding 30 degree axial sweep to the FEGV, adding bow/lean to the vane, and adding both sweep and bow/lean to the vane.

5) (See ***Figure 3-14*** where PS = pressure side of the airfoil, SS = suction side of the airfoil).

6) *Baseline Fan 1 radial vanes in forward position with simulated tip boot* – Shown in ***Figure 3-15***, this geometry approximation was intended to determine the effect on noise of forward sweeping the vane tip region by 45 degrees. This configuration was considered because of the predicted importance of the fan tip turbulence/FEGV interaction broadband noise source.

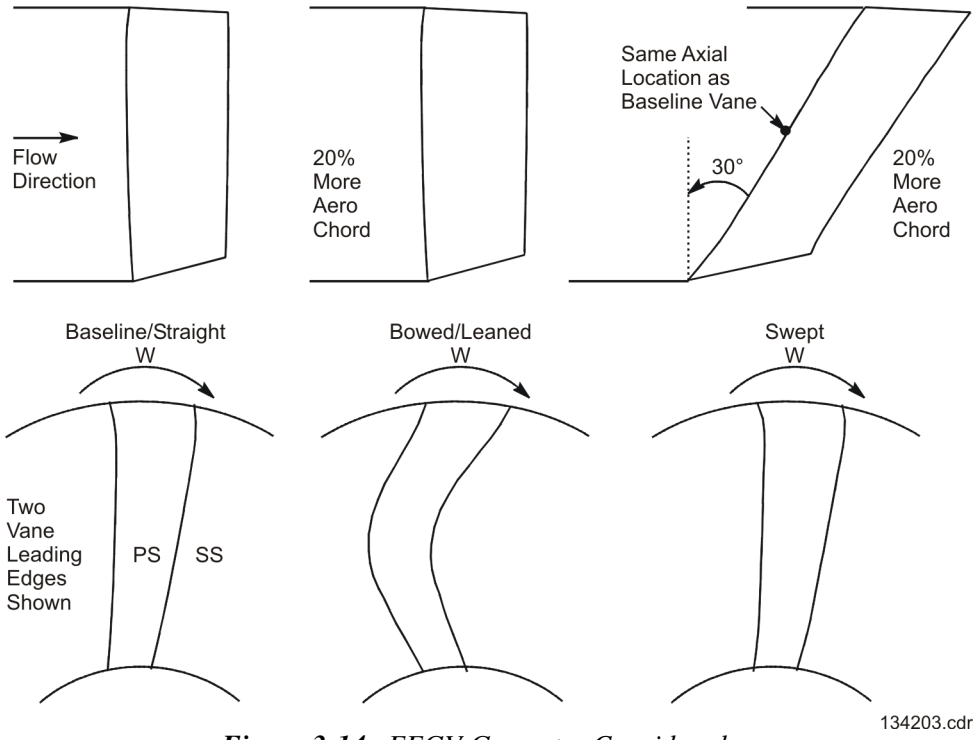

Figure 3-14. *FEGV Geometry Considered*

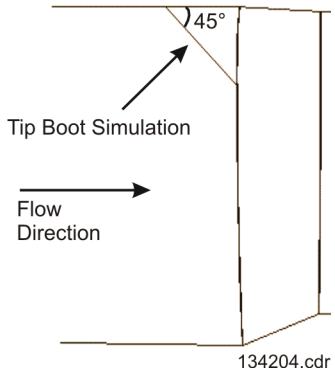

Figure 3-15. *Tip Boot Geometry*

All calculations were performed with the FEGV leading edge in the existing forward FEGV position on the rig (***Figure 2-22***).

For this design study, sideline, cutback, and approach, operating conditions were considered (see ***Table 2-1***). To perform FEGV acoustic studies, the fan noise design system was modified somewhat from that shown in ***Figure 2-19***. Instead, the design system shown in ***Figure 3-16*** was used. This system eliminates the running of the BFaNS and replaces it with the calculation of two empirical deltas:

- 30 log [cos(vane sweep angle)] – comes from Allison swept vane testing (Reference 12) and first order modeling.

- 7 log (vane number) – comes from Boeing rig testing and the BFaNS predictions.

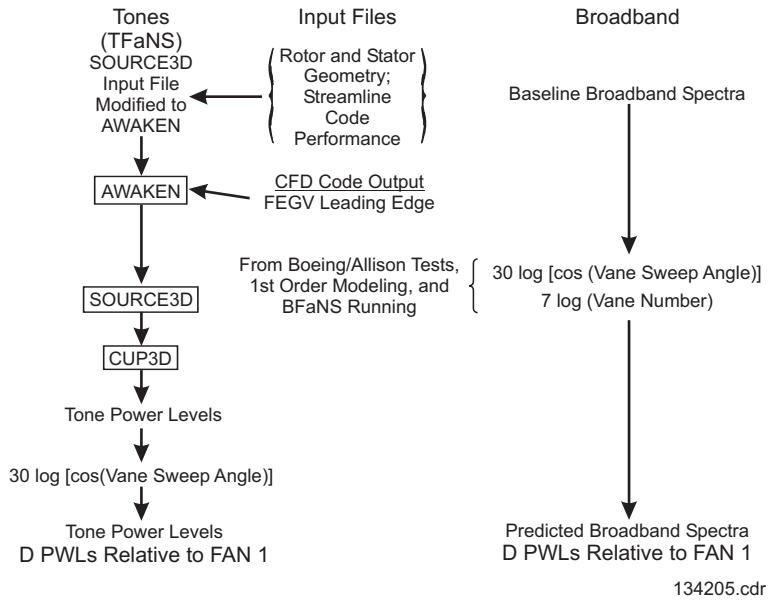

Figure 3-16. *Noise Design System for FEGV Study*

This modification permitted FEGV geometry to be analyzed for a wide range of vane numbers, thus allowing for more effective stator design. Tone noise was predicted using the same process that was used for the rotor design studies. The rotor and stator were coupled using a rotor wake/stator interaction noise source as the driver (***Figure 2-20***). Delta power levels from the baseline Fan 1 design were determined and added to Fan 1 data. EPNL predictions were then performed using the engine/aircraft configuration outlined in the beginning of Section 2.3.3. Cumulative EPNLs (sums of the three operating conditions) were calculated and compared to the baseline. Delta EPNLs were then created relative to the baseline Fan 1 design.

To predict BPF noise when it was cuton, inlet and aft BPF tone SPL directivity shapes from an existing full-scale engine were used for multiple low speeds. Sound power levels were also calculated for this full-scale engine for each speed. Measured normalized inlet and aft BPF SPL directivities were then calculated using the equation:

$$SPL_{NORM}\left(\theta, N_{1_C}\right) = SPL\left(\theta, N_{1_C}\right) - PWL\left(N_{1_C}\right)$$

where:

SPL_{NORM} = Normalized BPF sound pressure level, inlet and aft (dB)

SPL = Full-Scale BPF sound pressure level, inlet and aft (dB)

PWL = Full-Scale BPF sound power level, inlet and aft (dB)

N_{1c} = Function of corrected rotational speed

θ = function of farfield directivity angle.

Normalized BPF SPL directivity shapes, inlet and aft, were then combined and curve fitted. ADP 22-in. rig inlet and aft BPF SPL directivities were predicted by adding normalized directivities (from above) to the TFaNS predicted inlet and aft BPF power levels. The remainder of the system explained above was then used to calculate fan tone deltas and EPNLs.

The tip boot configuration predictions were made by using tone levels from the straight vane configuration. Broadband noise was then calculated by assuming that the fan tip turbulence/stator interaction noise source dominated. Thus, using 30 log [cos(sweep)] where sweep equals 45 degrees, we expect a 4.5 dB noise reduction. Assuming all other broadband noise sources are down about 10 dB, the noise reduction totals about 4.0 dB. This delta was applied to the broadband database before the result was flown.

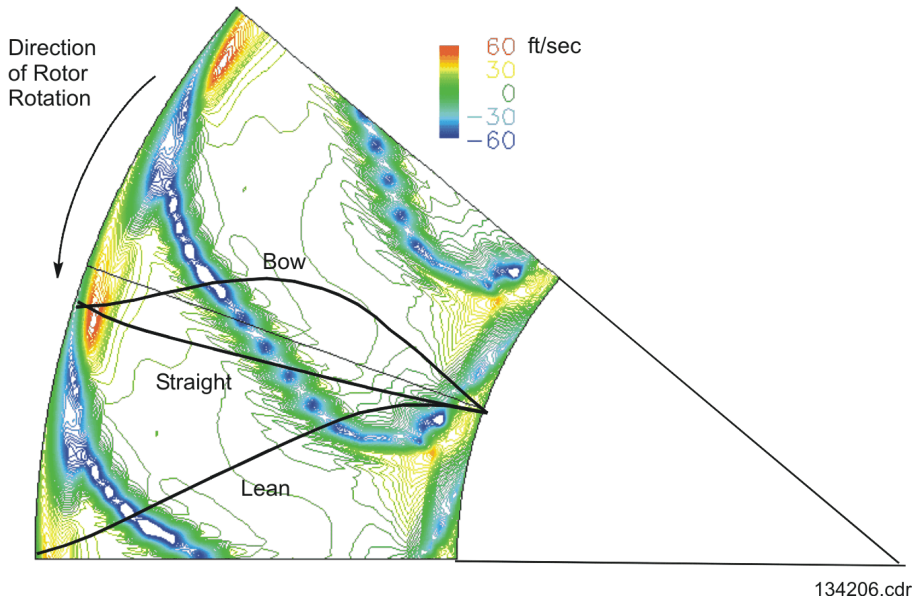

Figure 3-17. *CFD-Predicted Upwash Velocities with Cutback Power at the Straight Stator Leading Edge for ADP Fan Rig 1*

Figure 3-17 was used for the development of bow/lean designs. This figure shows the CFD predicted upwash velocities (*i.e.*, the velocities perpendicular to the average mean flow) at the baseline straight stator leading edge with cutback power. Assuming a zero incidence on a cascade of flat plate stators, these velocities indicate the type of unsteadiness encountered by the stator. The non-smooth shapes in the plot are a function of how the plotting routine interpolates the velocities from one grid point to the next. The direction of rotor rotation is noted as counterclockwise.

Figure 3-17 is useful in determining the phase of the wake across the span of the FEGVs. Potential vane leading edges were compared with this figure, including the present straight vane, leaned vane, and bowed vane possibilities. In ***Figure 3-17***, the three most promising configurations are considered a straight vane (the baseline), a leaned vane, and a bowed vane. If the FEGV and the wake are in line with each other, wake *slapping* occurs. This tends to cause high noise levels because the phase lag from radius to radius is zero. On the other hand, a vane that sweeps smoothly through the wake produces different radial phases and, usually, low tone noise. Each vane set considered was assessed qualitatively for the smallest amount of wake slapping.

The straight vane shows some phase lag from the midspan to the tip and near the hub. However, there is a section of the vane at about 30 percent span where the wakes *slap* the vanes. This is hypothesized to cause higher tone noise in this region that could be lowered. The leaned vane shows improved phasing from the midspan to the tip, but also suffers from vane *slapping* at about 30 percent span to the hub. The bowed vane shows no vane *slapping* anywhere across the vane. Thus, this bowed vane design was one of the design concepts considered in addition to the straight (baseline vane).

Vane sweep has been found to have a powerful effect on fan noise (Reference 12). This effect impacts both broadband and tones from the point of view of reducing the effective Mach number going into the stator. It also can lower noise by reducing the impact of vane *slapping,* as described in the bow/lean discussion, by changing the distance the wake must travel from hub to tip. Reference 12 found that at least 30 degrees of sweep is desirable to reduce noise. Thus, this concept was used as another method for reducing noise.

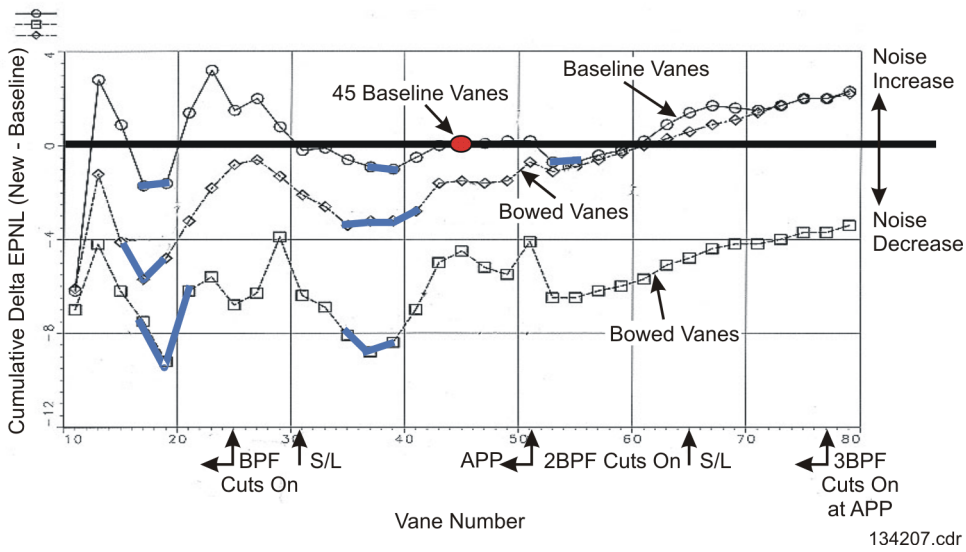

Figure 3-18. *Cumulative Delta EPNL (APP+C/B+S/L): Straight Versus Bowed Versus Swept Vanes*

The evaluation of the various vane geometries will now be discussed in the form of cumulative delta EPNLs relative to the Fan 1 baseline configuration. ***Figure 3-18*** shows cumulative delta EPNL predictions for the baseline, bowed, and swept vane geometries for vane numbers ranging from 11 to 79 vanes. The baseline Fan 1 rig has 18 fan blades and 45 FEGVs. The baseline FEGV prediction point is denoted by the red dot on the figure. At the bottom of ***Figure 3-18***, cuton vane number ranges are shown that correspond to BPF, 2BPF and 3BPF, from APP to sideline S/L powers. The specified harmonic remains cuton below these vane number ranges. The thick horizontal black line denotes no change from the baseline engine; below that line is a noise decrease and above that line is a noise increase.

A number of observations can be made about ***Figure 3-18***:

- The swept vanes produce the most noise reduction.
- This is, in part, due to the 30 log [cos(vane sweep angle)] used in the calculation of tones and broadband which, by itself, accounts for a 1.9 dB noise reduction at each operating condition. The maximum noise reductions are found for cuton vane numbers and are shown as thick blue lines.
- At high vane numbers, the noise goes up with increasing vane number linearly or near linearly. This is due to the 7 log (vane number) in the broadband noise model.
- Once 2BPF begins to cuton, then the effects of the tones become more noticeable.
- Varying vane number using the baseline vane geometry provides limited noise reductions. These are shown as thick blue lines on the baseline vanes curve. Noise reductions amount to less than three-quarters of a cumulative EPNL, relative to the baseline.
- The bowed vanes result in more noise reduction. This type of vane is best for cuton vane numbers. The low noise vane numbers are outlined along the bowed vane line as thick blue lines.
- The vane numbers where the most noise reduction can be obtained seem to surround the fan blade number (*i.e.*, vane numbers of around 15 to 19).
- Noise reductions can also be made for vane numbers around twice the number of fan blades (*i.e.*, 35 to 39 vanes)

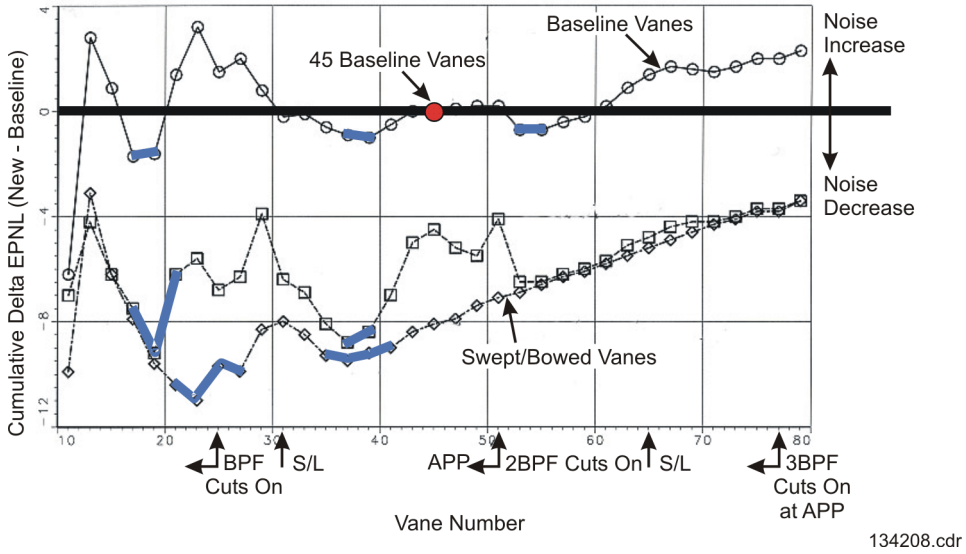

Figure 3-19. *Cumulative Delta EPNL (APP+C/B+S/L): Straight Versus Swept Versus Swept/Bowed Vanes*

Results for the baseline vanes, swept vanes (the best configuration in ***Figure 3-18***), and the swept and bowed vanes are shown in ***Figure 3-19***. This figure is configured in much the same fashion as ***Figure 3-18***. The following results can be stated from ***Figure 3-19***:

- The swept/bowed vane configuration shows the most noise reduction of all the cases shown so far.
- By sweeping and bowing the vanes, the design system essentially shows a 7 log (vane number) trend above approximately 37 to 39 vanes, which is consistent with the broadband noise prediction. Below this point, tone noise enters the total noise results.
- Maximum noise reduction potential appears to be a little above the 18 fan blade number (approximately 21 to 25 vanes) with a secondary minimum at 35 to 41 vanes.

It should be noted that for ***Figures 3-18*** and ***3-19,*** these noise reductions can be quite significant. The noise reductions are predicated on certain tone noise reductions based on rotor wake/stator interaction noise only. Broadband noise also follows certain assumptions regarding the importance of rotor turbulence/FEGV interaction noise sources relative to only fan noise sources. These assumptions may overpredict the overall noise reduction potential, though the trends appear reasonable. There appears to be some significant noise benefit possible with a swept/bowed FEGV.

The last vane configuration to be discussed is the tip boot. This is essentially the baseline vane with a modification in the tip region that reduces fan tip turbulence/FEGV interaction noise. Thus, this noise source is assumed to be dominant (which it appears to be in this rig). ***Figure 3-20*** shows this configuration along with the baseline configuration and the swept/bowed vane configuration. As before, maximum noise reduction vane numbers are shown as thick blue lines on this chart for each configuration.

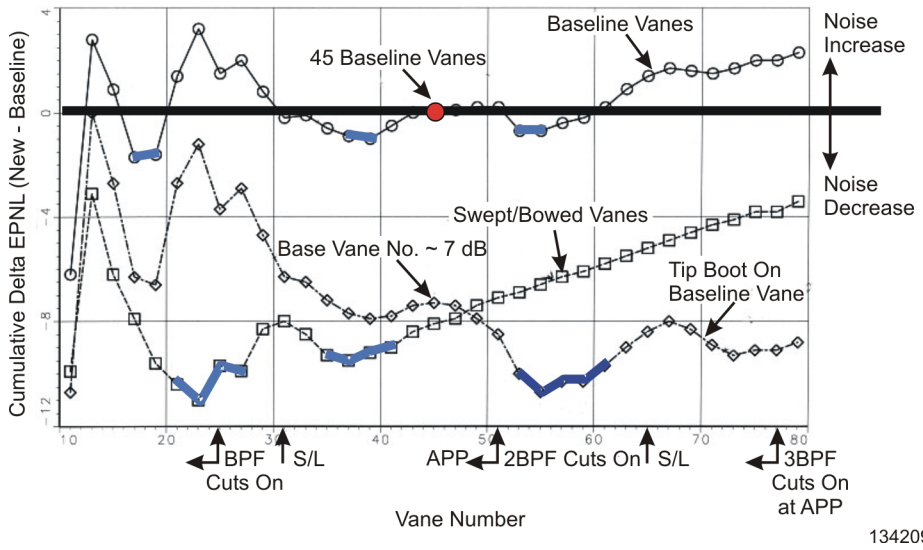

Figure 3-20. *Cumulative Delta EPNL (APP+C/B+S/L): Straight Versus Swept Versus Swept/Bowed Vanes*

Observations from ***Figure 3-20*** include:

- Both the swept/bowed vane and the tip boot appear to maximize the fan stages' noise reduction potential, given the optimum vane numbers for each configuration.
- The tip boot only works on broadband dominated vane numbers, assuming fan tip turbulence/FEGV interaction is the noisiest broadband noise source. Thus, it is optimum at the higher vane numbers (approximately 53 to 61 vanes). The swept/bowed configuration works best when tones contribute, and makes vane numbers on the order of 21 to 25 vanes the quietest.
- The contribution of 3BPF is seen more clearly for the tip boot configuration, since broadband noise has been dropped an additional 4dB per operating condition due to the tip boots.
- Tip boots do lower noise at lower vane numbers, just not as effectively as sweep and bow or lean, since tone noise dominates at lower vane numbers.

Table 3-4 summarizes the potential noise reduction that can be obtained from the FEGV geometries studied. The optimum vane numbers for each configuration are also given based on ***Figure 3-18***, ***Figure 3-19***, and ***Figure 3-20***. The noise reductions quoted are based on the assumptions made about the noise. Thus, it is likely that some of the noise reduction will be lost due to other noise sources. However, significant noise reduction potential does exist with properly designed FEGVs.

Table 3-4. *Optimum Vane Numbers and Noise Reduction Potential for FEGV Configuration*

Configuration	***Noise Reduction (Cumulative EPNdB)***	***Optimum Vane Numbers***
Baseline Straight Vane	~1 EPNdB	17 to 19, 35 to 41, 53 to 55
Bowed Vane	~2 to 4 EPNdB	15 to 19, 35 to 41
30 Degree Swept Vane	~6 to 8 EPNdB	17 to 19, 35 to 39
Bowed +30 Degree Swept Vane	~8 to 10 EPNdB	21 to 25, 35 to 41
Tip Boot Added to Baseline	~8 EPNdB	53 to 61 (at the baseline, 45 vanes: 7 EPNdB cum)

3.3 STRUCTURAL ANALYSIS OF THE SELECTED FEGV CONFIGURATION

A preliminary structural assessment of the 22 vane, bowed +30.5 degree swept FEGV configuration that showed significant noise reduction potential (see ***Table 3-4***),was performed to determine this configuration's stiffness and deflection characteristics relative to the 52-vane configuration of Fan 1. This back-to-back nacelle stiffness check was conducted to verify that acceptable fan blade tip clearances would exist under test facility loads.

The existing finite element model of the 22-in. fan/nacelle test rig provided the baseline configuration. The new FEGV configuration was developed from an airfoil shape representing the bowed/swept configuration and incorporated into the model. Back-to-back finite element stiffness checks were performed for both rig configurations. Stiffness results were tabulated.

3.3.1 Finite Element Results

The original ANSYS models obtained by archival retrieval were converted into MSC/NASTRAN V68 files. The translator used was FEMAP V5.0. All analyses were performed using MSC/NASTRAN V68.

The models were constrained at the FEGV I.D. rear. A unit load of 1,000 lbf was applied in the nacelle at the fan tip location for each coordinate direction. This would allow for stiffness comparison of the original and bowed/swept configurations. Geometry and material definition was copied for the 22-vane model. In each FEGV model, the FEGVs were modeled with steel properties. Deflection results were recorded and are organized in ***Table 3-5***.

Nomenclature

The cylindrical coordinate system was used:

- x – a direction radially from the rig centerline
- θ – a direction tangential to the radial direction and perpendicular to the rig centerline
- z – a direction along the rig centerline.

Table 3-5. *Finite Element Results Summary*

Deflection Data	***Original 52-Vane Configuration***	***Bowed/Swept 22-Vane Configuration***	***Percent Stiffness Increase***
Coordinate Direction	(in. × 1,000)	(in. × 1,000)	|(orig - new)|/orig × 100
x (Transverse)	2.227	2.163	+2.9
θ (Torsional)	36.072	9.226	+74.4
z (Axial)	2.459	0.691	+71.9

All deflection data was taken at Node 10886, which is at the midspan fan blade tip, 170 in. axial location.

Stress results are not provided for two reasons; the program was terminated early and stresses were not critical to the preliminary study.

3.3.2 Discussion of Results

The analysis shows the 22-vane configuration is significantly stiffer than the original configuration in the torsional and axial directions and only slightly stiffer in the transverse direction. The results indicate the new configuration would be suitable for operation in the rig. Finite element stresses were not tabulated.

The structural analysis work described in this section was performed by FTS Inc. at 144 Main Street, Unit D, East Hartford, CT, 06118, under subcontract to P&W.[1] References 13 through 16 list significant information transfers from P&W to FTS. Results were reported in FTS Report No. 8A-002.

[1] Reference job request No. 98-AST-002.

3.3.3 Finite Element Figures

Figures 3-21 through ***3-26*** show the modeling element breakup used in the analysis. These figures are presented so that comparisons of the bowed/swept 22-vane configuration to the baseline 52-vane configuration are straightforward.

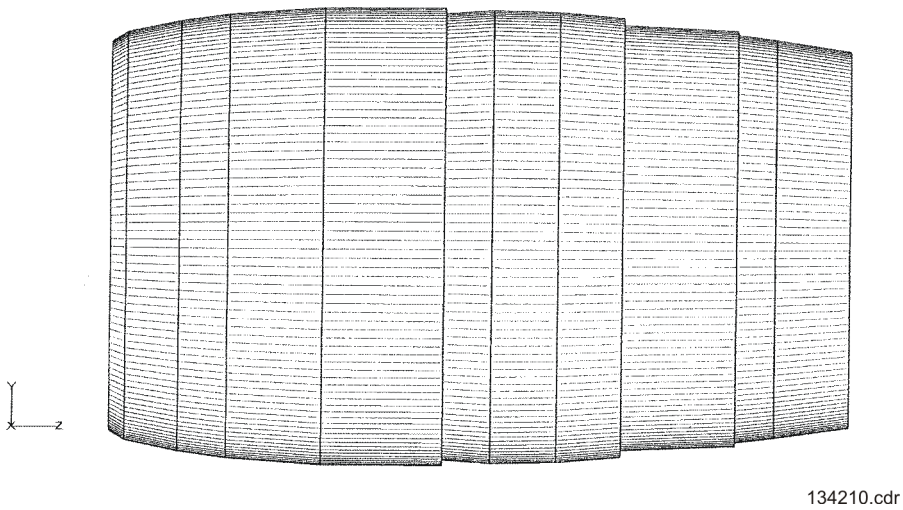

Figure 3-21. *Nacelle/FEGV 52-Vane Configuration Side View*

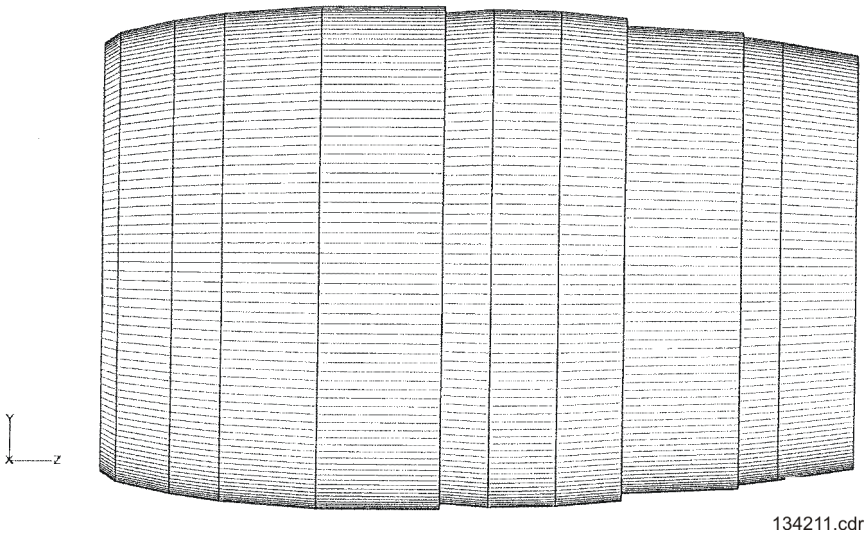

Figure 3-22. *Nacelle/FEGV 52-Vane Configuration Side View*

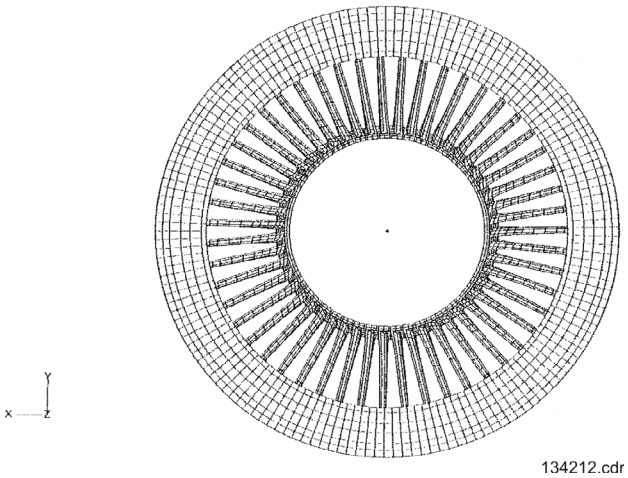

Figure 3-23. *Nacelle/FEGV 52-Vane Configuration Front View*

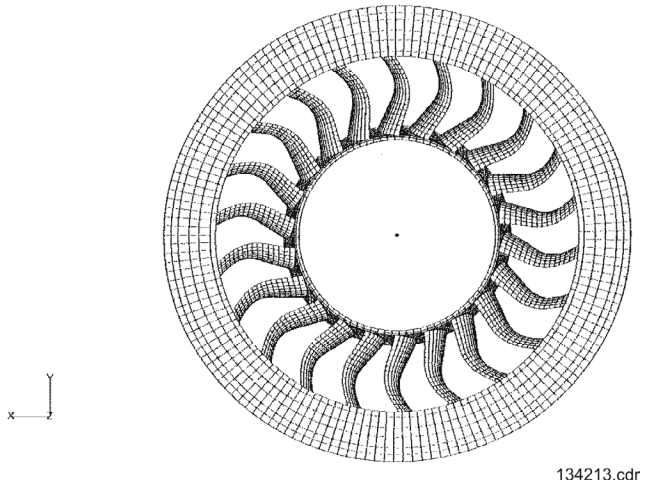

Figure 3-24. *Nacelle/FEGV Bowed/Swept 22-Vane Configuration Front View*

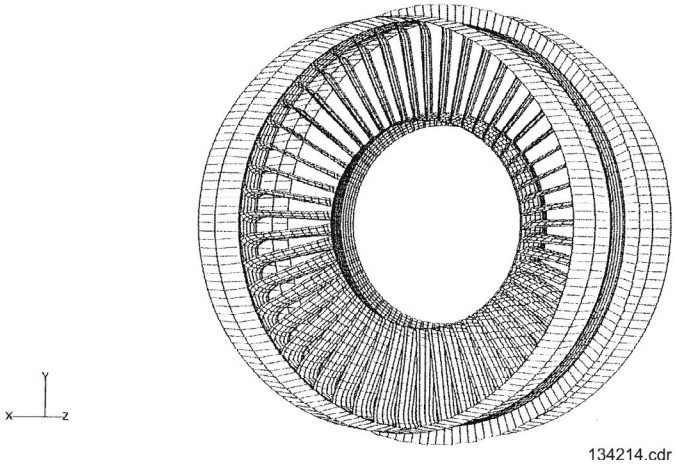

Figure 3-25. *FEGV 52-Vane Configuration Section View*

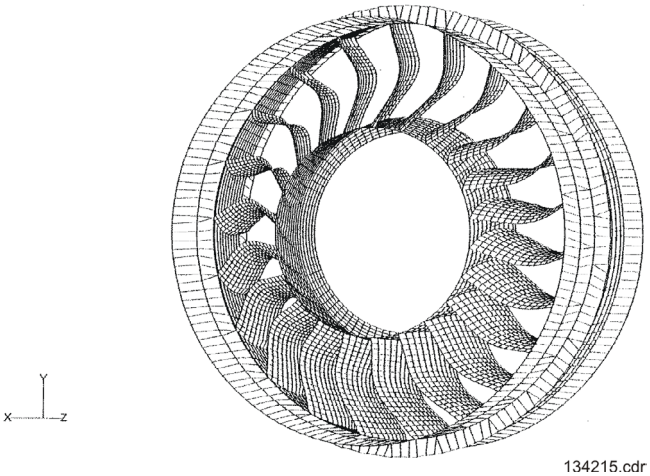

Figure 3-26. *FEGV Bowed/Swept 22-Vane Configuration Section View*

4. CONCLUSIONS

This task was originally authorized to design and build the third (Fan 3) in a series of 22-in. diameter tip fan rigs for testing at NASA GRC. The design of Fan 3 was intended to incorporate experience gained from Fans 1 and 2 and demonstrate noise reduction technology that would surpass accepted 1992 levels by 6 dB.

Midway through the program, NASA decided to cancel the design, fabrication, and testing phases of the work. The scope of the program changed accordingly to concentrate on two subtasks:

1. Rig data analysis and CFD code validation
2. Fan and FEGV optimization studies.

4.1 CFD AND FAN NOISE DESIGN SYSTEM VALIDATION CONCLUSIONS

A noise prediction system is in place and integrated with CFD. The CFD tool predictability has been assessed to gain understanding of fan noise sources, such as wakes and turbulence. The resulting tool predicts well 3-D flowfield features from the blade trailing edge to about a chord downstream. However, the CFD tool loses accuracy as the distance from the trailing edge increases beyond a blade chord. The comparisons of CFD predictions to data hinge on several assumptions. These assumptions encompass any modeled geometric discrepancies with actual geometry, modeled inlet turbulence profiles, modeled turbulence transition, and modeled fan/core flow split with test.

The comparisons of noise predictions to rig test data showed that both the TFaNS and the BFaNS demonstrated reasonable agreement with the data to the degree that these tools can reliably be used for design work.

4.1.1 Rig Data Analysis

Fan 1 and 2 test data were analyzed for noise differences. This analysis found that the expected 2 dB noise reduction for Fan 2 was not realized. The scaling rules used for this prediction were:

- The standard 50 log (tip speed) scaling factor for the reduced tip speed of Fan 2, which indicated a reduction of 2.5 dB
- The empirical 7 log (vane number) scaling factor from Boeing rig testing for broadband noise, which predicted a 0.4 dB increase.

The result was a net 2 dB BFaNS reduction. When using the BFaNS to evaluate Fan 2, the results confirm a noise increase on the order of 2 dB. The results show that the scaling rules initially used do not apply to the different aerodynamic loading of these two fans.

The **section** on rig airflow and inlet separation analysis describes the method used to determine total fan airflow and shows the good agreement of predicted boundary layer profiles to measured profiles. The results of the inlet flow separation studies show separation angles-of-attack ranging from 29.5 degrees to 27 degrees for the range of airflows tested.

4.1.2 Fan Optimization Studies

Five aerodynamic rotor configurations were included in a parametric study to investigate the effects of fan loading distribution on fan noise. The results of the studies were significant in leading to the decision not to pursue a new rotor design for Fan 3. Noise predictions for a 750 ft/sec Fan 3 rotor showed little reduction in comparison to Fan 2, and resulted in the recommendation to concentrate efforts on FEGV stator designs.

4.1.3 FEGV Optimization Studies

The parametric study on FEGV designs included variations on

1. Vane numbers
2. Solidity (chord change)
3. Stacking line variations including sweep, bow, and lean
4. Vane tip boots.

The study results showed the potential for 8 to 10 EPNdB noise reduction relative to the baseline, with the configuration featuring 22 bowed vanes, each with 30 degrees of sweep, showing the greatest potential.

A preliminary rig nacelle structural analysis was performed on the 22-vane configuration that is bowed with 30 degrees of sweep relative to the 52-vane configuration of Fan 1. The results showed the 22-vane configuration to be significantly stiffer than the original in the torsional and axial directions and only slightly stiffer in the transverse direction. Stress results were not determined, since this part of the program was cancelled.

5. REFERENCES

1. Rhie, Chae M., *et al*, "Development and Application of a Multistage Navier-Stokes Solver Part 1: Multistage Modeling Using Bodyforces and Deterministic Stresses," ASME 95-GT-342.
2. LeJambre, C.R., *et al*, "Development and Application of a Multistage Navier-Stokes Solver Part 2: Application to a High Pressure Compressor Design," ASME 95-GT-343.
3. Chima, R.V., "A K-W Turbulence Model for Quasi-Three-Dimensional Turbomachinery Flows," AIAA 96-0248, January 1995.
4. Topol, D.A., "Tone Fan Noise Design/Prediction System, Volume I: System Description, CUP3D Technical Documentation and Manual for Code Developers," NASA-CR-1999-208882, March 1999.
5. Topol, D.A., "Tone Fan Noise Design/Prediction System, Volume II: User Manual, TFaNS, Version 1.4," NASA-CR-1999-208883, March 1999.
6. Topol, D.A., "Tone Fan Noise Design/Prediction System, Volume III: Evaluation of System Codes," NASA-CR-1999-208884, March 1999.
7. Meyer, H.D., "Source Methodology for Turbofan Noise Prediction (SOURCE3D Technical Documentation)," NASA-CR-1999-208877, March 1999.
8. Glegg, S.A.L., "Broadband Noise from Ducted Prop Fans," AIAA 93-4402, October 1993.
9. Glegg, S.A.L., "Airfoil Self Noise Generated in a Cascade," AIAA 96-1739, May 1996.
10. Glegg, S.A.L. and Jochault, C., "Broadband Self Noise from a Ducted Fan," May 1997.
11. Neubert, R., Bock, L., Malmbourg, E., Owen-Peer, W., "Advanced Low-Noise Research Fan Stage Design," NASA CR-97-206308, December 1997.
12. Woodward, R.P., Elliot D.M., Hughes, C.E., and Berton, J.J., "Benefits of Swept and Leaned Stators for Fan Noise Reduction," NASA TM-TBD, October 1997.
13. W. Brockett to E. Canal, "Structural and Mechanical Design Subcontract Effort," P&W internal correspondence, dated 17 December 1997.
14. W. Brockett to Distribution, "Transmittal of Bowed/Swept Vane FEM Mesh," P&W coordination memorandum, dated 12 February 1998.
15. K. Winckel to Distribution, "Transmittal of Structural Analysis Files to FTS," P&W coordination memorandum, dated 3 March 1998.
16. D. Mathews to Distribution, "Third Build of 22-in. ADP Fan Stage Will Be Canceled," P&W internal correspondence, dated 30 April 1998.
17. Hobbs, D.E., Malmborg, E.W., Neubert, R.J., Philbrick, D.H., "Low Noise Research Fan Stage Design," NASA Contract Report 195832, March 1995.

REPORT DOCUMENTATION PAGE

Form Approved
OMB No. 0704-0188

1. AGENCY USE ONLY (*Leave blank*)	2. REPORT DATE	3. REPORT TYPE AND DATES COVERED
	February 2004	Final Contractor Report

4. TITLE AND SUBTITLE

Advanced Subsonic Technology (AST) 22-Inch Low Noise Research Fan Rig Preliminary Design of ADP-Type Fan 3

5. FUNDING NUMBERS

WBS–22–781–30–12
NAS3–27727

6. AUTHOR(S)

David A. Topol, Clint L. Ingram, Michael J. Larkin, Charles H. Roche, and Robert D. Thulin

7. PERFORMING ORGANIZATION NAME(S) AND ADDRESS(ES)

United Technologies Corporation
Pratt & Whitney
East Hartford, Connecticut 06108

8. PERFORMING ORGANIZATION REPORT NUMBER

E–14242

9. SPONSORING/MONITORING AGENCY NAME(S) AND ADDRESS(ES)

National Aeronautics and Space Administration
Washington, DC 20546–0001

10. SPONSORING/MONITORING AGENCY REPORT NUMBER

NASA CR—2004-212718

11. SUPPLEMENTARY NOTES

David A. Topol, Clint L. Ingram, and Michael J. Larkin, United Technologies Corporation, Pratt & Whitney, East Hartford, Connecticut 06108; and Charles H. Roche and Robert D. Thulin, FTS, Inc., East Hartford, Connecticut 06108. Project Manager, Robert J. Jeracki, Structures and Acoustics Division, NASA Glenn Research Center, organization code 5940, 216–433–3917.

12a. DISTRIBUTION/AVAILABILITY STATEMENT

Unclassified - Unlimited
Subject Category: 02 Distribution: Nonstandard

Available electronically at http://gltrs.grc.nasa.gov

This publication is available from the NASA Center for AeroSpace Information, 301–621–0390.

12b. DISTRIBUTION CODE

13. ABSTRACT ***(Maximum 200 words)***

This report presents results of the work completed on the preliminary design of Fan 3 of NASA's 22-inch Fan Low Noise Research project. Fan 3 was intended to build on the experience gained from Fans 1 and 2 by demonstrating noise reduction technology that surpasses 1992 levels by 6 dB. The work was performed as part of NASA's Advanced Subsonic Technology (AST) program. Work on this task was conducted in the areas of CFD code validation, acoustic prediction and validation, rotor parametric studies, and fan exit guide vane (FEGV) studies up to the time when a NASA decision was made to cancel the design, fabrication and testing phases of the work. The scope of the program changed accordingly to concentrate on two subtasks: (1) Rig data analysis and CFD code validation and (2) Fan and FEGV optimization studies. The results of the CFD code validation work showed that this tool predicts 3D flowfield features well from the blade trailing edge to about a chord downstream. The CFD tool loses accuracy as the distance from the trailing edge increases beyond a blade chord. The comparisons of noise predictions to rig test data showed that both the tone noise tool and the broadband noise tool demonstrated reasonable agreement with the data to the degree that these tools can reliably be used for design work. The section on rig airflow and inlet separation analysis describes the method used to determine total fan airflow, shows the good agreement of predicted boundary layer profiles to measured profiles, and shows separation angles of attack ranging from 29.5 to 27° for the range of airflows tested. The results of the rotor parametric studies were significant in leading to the decision not to pursue a new rotor design for Fan 3 and resulted in recommendations to concentrate efforts on FEGV stator designs. The ensuing parametric study on FEGV designs showed the potential for 8 to 10 EPNdB noise reduction relative to the baseline.

14. SUBJECT TERMS

Wind tunnel; Powered model; Scale model; Turbofan; Fan; Ducted fan; Vane; Stator; Outlet guide vane; Turbomachinery; Noise; Fan noise; Low noise; Noise prediction

15. NUMBER OF PAGES

63

16. PRICE CODE

17. SECURITY CLASSIFICATION OF REPORT	18. SECURITY CLASSIFICATION OF THIS PAGE	19. SECURITY CLASSIFICATION OF ABSTRACT	20. LIMITATION OF ABSTRACT
Unclassified	Unclassified	Unclassified	